# European design approaches for isolated cold-formed thin-walled beam–columns with mono-symmetric cross-section

Claudio Bernuzzi [a], Marco Simoncelli [b,*]

[a] *Department of Architecture, Built Environment and Construction Engineering, Politecnico di Milano, Milano, Italy*
[b] *Department of Civil Engineering and Architecture, Università di Pavia, Pavia, Italy*

Received 12 May 2014
Revised 22 December 2014
Accepted 27 December 2014

## 1. Introduction

Thin-walled cold-formed member structures are widely used in aerospace, automobile and civil and architecture industries [1]. Among the various advantages, mainly associated with the relatively simple and very cheap techniques required for their production and shaping, it is important to mention the relevant high strength to weight ratio. One of the most important uses of this type of steel members is for steel storage pallet rack structures (Fig. 1), which became increasingly complex in the recent years with a large number of bays and beam levels to support heavy storage loads [2,3]. Key rack components are the uprights (vertical members), which present generally a mono-symmetric cross-section (Fig. 2), beams (pallet beams or stringers) and bracing diagonals (lacings) connecting the uprights to each other in the cross-aisle direction to form the upright frames. All the connections between the uprights and the pallet beam (beam-to-column joint) and the upright ends and the industrial floor (base-plate connections) are usually partial strength semi-rigid joints; therefore the design has necessarily to be developed adopting the semi-continuous frame model [4].

Because of the differences in the shape of the cross-section of the structural components and in the connection types, technical information in addition to the ones provided by the standard provisions for the more traditional thin-walled steel structures is required. Refined codes of practice [5–10] are now available for routine design, which have been recently updated and significantly improved but few important aspects need additional investigations to further increase the safety level guaranteed by the routine rack design rules.

Owing to the extensive use of mono-symmetric cross-section uprights, the shear center is often non-coincident with the centroid: special attention is hence required in the structural analysis phases as well as in the subsequent member verification checks. Despite very refined formulations that are nowadays available [11–24] proposing beam elements for linear and non-linear analy-sis to accounting for material and geometrical non-linearity,

* Corresponding author. Tel.: +39 3312864026.
*E-mail address:* dott.marcosimoncelli@gmail.com (M. Simoncelli).

designers generally model all types of steel storage racks via Finite Element (FE) analysis packages characterized by 6 degrees of freedom (DOFs) beam formulations [25–27], which are inadequate for racks because of the absence of the Wagner coefficients and of the shear center eccentricity in both elastic and geometric stiffness matrix. It should be noted that rarely bi-symmetric cross-section members are used as uprights for medium-rise racks. Based on the authors' knowledge, in Italy only one manufacturer offers hol-low square members in the market. If reference is made to cladding racks (i.e. to ware-houses), which are out of the scope of the present paper, in several cases uprights have by-symmetric cross-section, owing to the high performance required, especially in seismic zones.

Few FE analysis programs [28–32] are nowadays available offering some of the already introduced refined beam formulations, adequate to represent the complex behavior of mono-symmetric cross-sections: in total 7 DOFs per each node of the beam element are hence necessarily required (Fig. 3b): 3 displacements ($u_o$, $w_s$ and $v_s$), 3 rotations ($\varphi_x$, $\varphi_y$, and $\varphi_z$) and the warping function $\theta$ (i.e. the 7th DOF), that is defined as:

$$\theta = \theta(x) = -\frac{d\varphi_x}{dx} \tag{1}$$

Warping effects are extremely important, influencing significantly the distribution of internal forces and moments on members and joints, the set of horizontal displacements and buckling modes of the overall rack [33–37] for static as well as for seismic design. No practical indications on the minimum requirements for the structural analysis tools nor design examples are available in rack design standards. A very limited attention has been paid to the development of benchmarks for open-mono-symmetric cross-section members: references [38,39] should be considered despite the fact that they deal with cross-sections significantly different from the ones currently used in rack practice. Furthermore, verifica-tion criteria in accordance with EN 15512 ignore for routine design

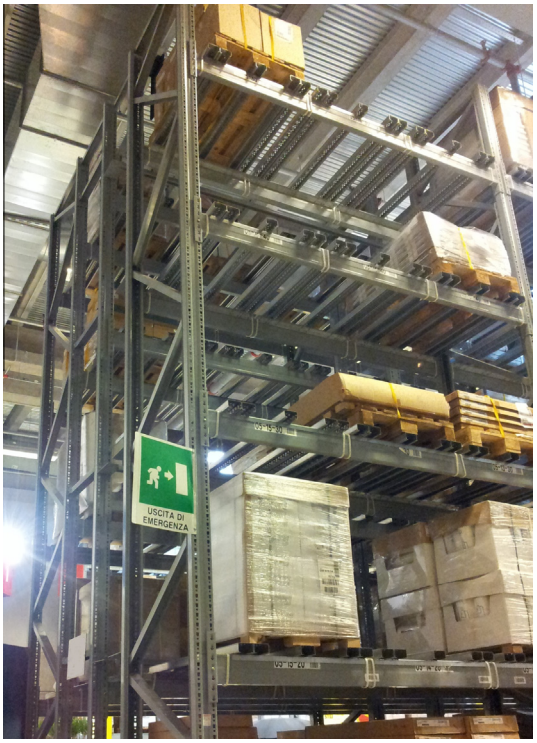


**Fig. 1.** Typical selective steel storage pallet rack.

**Fig. 2.** Typical mono-symmetric cross-section employed as rack uprights.

the key features associated with the presence of only one axis of symmetry and the coupling between flexure and torsion is considered for the sole evaluation of the critical elastic buckling load of isolated compressed columns in spite of clear indications provided in Eurocode, as discussed in [36].

A research study is currently in progress in Italy, in conjunction between the Politecnico di Milano and the University of Pavia, on the design rules currently adopted for steel storage pallet racks: final aim is to propose few essential improvements to increase the safety level of the racks. The general purpose FE analysis pro-gram for academic use NONSAP [40] was in the years modified in order to model semi-continuous steel frames accounting for sec-ond order effects and buckling analysis. Recently, an adequate FE 7 DOFs beam formulation including warping has been developed [41] and implemented in the updated version, named Ś iva [42], able to capture the complex response of pallet and drive-in racks, as well as of all the framed systems with mono-symmetric cross-section members. Authors decided to use this quite old (but extre-mely efficient) open-source software not only for economic rea-sons (no direct costs for the use of Ś iva) but also because, in some cases, the available refined 7 DOFs beam formulations imple-mented in the aforementioned commercial software programs do not allow to model complex cross-section geometries, like the ones in Fig. 2, or they did not pass positively [43] all the several bench-mark tests taken from literature on cases of interest for rack practice.

This paper focuses on the influence that the interaction between flexural–torsional and lateral–torsional buckling modes plays on the upright load carrying capacity. Traditional design pro-cedures neglect this type of interaction, or consider it in a very simplified way, as well as the warping influence on the buckling behavior of beam–columns and on the overall static and seismic response of the whole rack. The degree of accuracy of the European routine design approaches for isolated beam–column members is herein considered: reference is made to members differing for cross-section geometry, slenderness and load conditions. Rack pro-visions [5] together with the design codes for thin-walled [44] and the general one for every type of steel members [45] are briefly introduced and applied in order to single out the benefits associated with the quite different approaches admitted in Europe for rack design. Research outcomes have been proposed on the basis of the results of 1296 design cases, comprising also the presence of the sole axial force or the sole bending moment. No attention is herein directly paid to the seismic design [8–10], despite that the proposed research outcomes should however be directly used also to guarantee adequate safety levels under earthquakes, deal-ing with the stability verification checks independently from the nature of the loads.

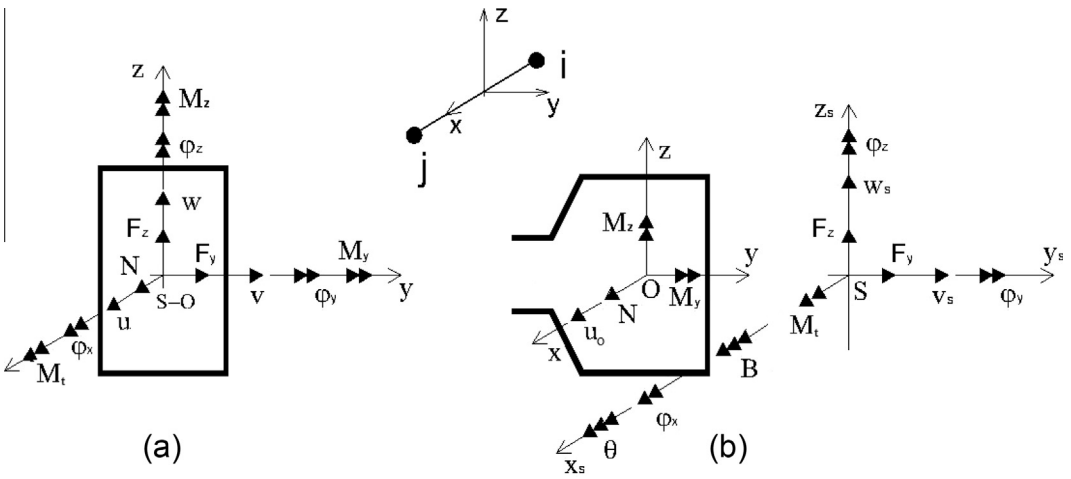


**Fig. 3.** Nodal displacements and internal forces for a beam element with 6 DOFs (a) or 7 DOFs (b) for each node.

## 2. The parameters considered in the study

Upright cross-sections usually belong to class 3 or 4, in accordance with the classification criterion proposed in part 1-1 of Eurocode 3 [45]: the design verification rules refer to the elastic performances (class 3) of the cross-section, eventually reduced (class 4) in terms of effective area, second moments of area and section moduli in accordance with the approaches related to the design assisted by testing [5–7]. For simplicity, in the following only class 3 cross-section members are considered, neglecting hence the reduction of the gross cross-section due to local and distortional buckling phenomena and to their mutual interaction. The presence of perforations is not considered, i.e. attention is focused on uprights with solid cross-section, which are typical of selective not adjustable storage systems, because the focus of the present paper is the comparison between the admitted design approaches.

The four upright cross-sections presented in Fig. 4 have been selected. For each of them, the ratio between the second moments of area ($I_y/I_z$), the section moduli ($W_y/W_z$) and radii of gyration ($\rho_y/\rho_z$) are presented in Table 1, together with the ratio $y_0/d$, i.e. the distance between the shear center and the centroid ($y_0$) over the distance between the centroid and the web ($d$). Furthermore, in order to allow a general appraisal of the guaranteed performances, the Saint Venant's torsional constant and the warping second moment of area ($I_t$ and $I_w$, respectively) and the maximum value of the first moment of the sectorial area ($\omega_{max}$) are reported in the same table, together with the squash load ($A \cdot f_y$) and the first yielding (elastic) moment ($W_y \cdot f_y$) of the gross cross-section. No additional data such as the complete geometry of the cross-section has been possible to present more in details because of the confidentiality required from manufactures on their commercial products. It should be noted that the considered cross-sections are

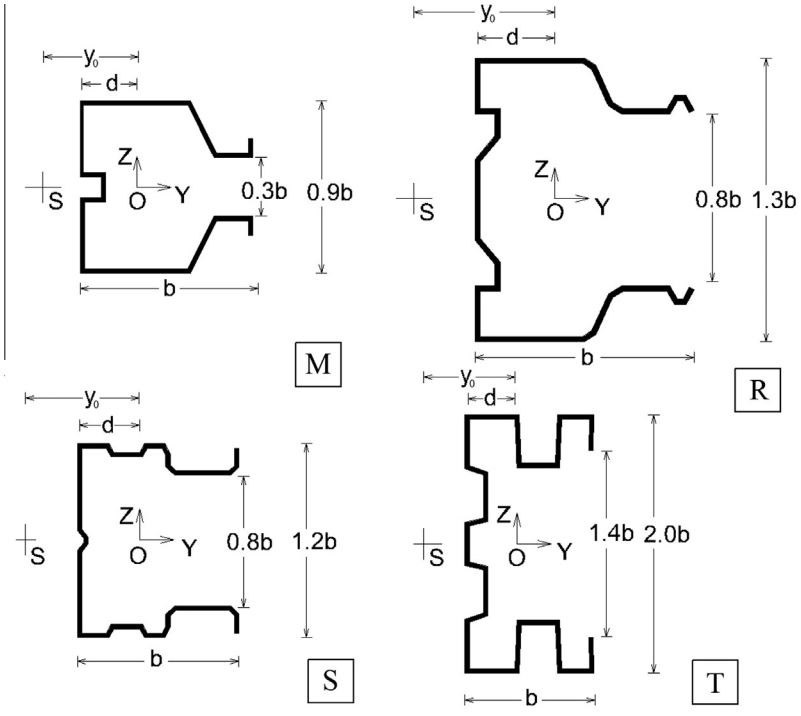


**Fig. 4.** The upright cross-sections considered in the present study.

**Table 1**
Key geometric parameters of the considered upright cross-section.

| | M | R | S | T |
|---|---|---|---|---|
| $A{\cdot}f_y$ [kN] | 2.03E+02 | 3.50E+02 | 1.78E+02 | 2.59E+02 |
| $W_y{\cdot}f_y$ [kN m] | 4.37 | 13.00 | 4.78 | 8.14 |
| $I_y/I_z$ | 0.992 | 2.194 | 1.809 | 4.709 |
| $\rho_y/\rho_z$ | 0.996 | 1.481 | 1.345 | 2.170 |
| $W_y/W_{z,sup}$ | 1.233 | 2.241 | 1.862 | 2.990 |
| $W_y/W_{z,inf}$ | 0.838 | 1.134 | 1.104 | 1.793 |
| $y_0/d$ | 2.306 | 2.253 | 2.296 | 1.989 |
| $I_t$ [mm$^4$] | 6.19E+02 | 2.05E+03 | 5.23E+02 | 9.72E+02 |
| $I_w$ [mm$^6$] | 1.60E+09 | 5.64E+09 | 5.94E+08 | 6.30E+08 |
| $\omega_{max}$ [mm$^2$] | 3.25E+03 | 8.20E+03 | 1.57E+03 | 1.58E+03 |

sufficiently representative of the most common geometries of uprights typically employed for medium-rise pallet racks. In particular, the ratio between the second moments of area ranges from 1.0 to 4.7, approximately, including the cases of symmetry axis corresponding to the major axis of the cross section, which is the most common situation in rack practice. It should be noted that M_upright presents values of $I_y/I_z$ and $\rho_y/\rho_z$ ratio approximately equal to the unity, but its response is significantly different from the one of by-symmetric cross-section members owing to the presence of a non-negligible shear center eccentricity.

Although pallet racks are spatial structures, major standard codes [5–7] admit for the routine design, the simplification of the spatial rack in a set of plane frames lying in the vertical planes, parallel and perpendicular to the aisles, each of which is initially considered to operate independently. As a consequence, in the following the reference is made to the case of beam–column under uniaxial bending and moments have been applied at the member ends about the symmetry axis, in order to refer the design verification to the down-aisle rack response, which is the most severe load condition for design purposes. Axial load was considered constant along the element acting together with a gradient moment expressed by means of parameter $\psi$, defined as the ratio between the maximum and the minimum end moment (Fig. 5). Eccentricity ($e$) of the axial load with respect to the centroid axis has been considered by selecting values ranging from zero (column) to infinity (beam) and reference is made to three different values of the effective length ($L$ = 1 m, 2 m and 3 m). Furthermore, three different restraint types have been considered for lateral buckling, via the effective length factors $k$ and $k_w$ accounting for rotation and warping of the ends of the member, ranging from 0.5 to 1.0.

The layout of all the considered cases in this parametric study is presented in Fig. 6.

## 3. Buckling interaction between axial load and bending moment

Overall member instability plays a rule of paramount importance in the design of steel structures, and in particular, in case of uprights of storage pallets racks. Owing to the presence of semi-rigid connections (beam-to-column and base-plate joints), non-negligible bending moments are transferred to uprights both in the down- and in the cross-aisle directions and hence verifica-tion of members under pure compression is limited to the diago-nals of the upright frames and of the bracing systems, when placed in the down-aisle direction, as it typically happens in seis-mic zones. The design of beam–columns is based on the principle of the equivalent slenderness and, as shown in the following sub-chapters, it strictly depends on the elastic buckling loads. In modern steel provisions it is required to evaluate the axial critical load of the columns ($N_{cr}$) and the lateral buckling moment of the beams ($M_{cr}$). Well-established equations are proposed in literature [38,46,47], which are shortly summarized in the Appendix A. With reference to the beam buckling, suitable numerical coefficients are defined to account for the bending moment distribution ($C_1$), load height effect ($C_2$) and the non-symmetry of the cross-section, $C_3$ (Wagner's coefficient). Differences can be observed in the $C$ coeffi-cient values proposed by design codes and several studies [48–50] have been recently executed to define them more accurately. Owing to the considered cases discussed in this paper (Fig. 6), only $C_1$ coefficient is of interest, being the flexure due to bending moments directly applied at the member end ($C_2$ = 0) and about its axis of symmetry ($C_3$ = 0). The values of $C_1$ herein considered are presented in Table A.1 of the Appendix A: reference is made to the contents of the Annex F of the previous version (ENV ver-sion) of EC3 [51]. No attention is paid in the present paper to the very important problem of the definition of more accurate values of the $C$ coefficients; furthermore, it is worth to mention that, the proposed research outcomes are however independent from the adopted $C_1$ values being all the results associated with the admit-ted design alternatives presented in comparative terms. As to beam–columns, the interaction between the axial and the lateral buckling load is currently neglected from the design point of view and extremely simplified assumptions are adopted, despite its rel-evant influence. Fig. 7 presents the typical bending moment–axial load buckling domain ($N_{cr}$–$M_{cr}$) together with the simplified buck-ling domain assumed both by rack [5] and cold-formed European design code [40], which leads to overestimate very significantly the elastic buckling resistance. Furthermore, it should be noted that closed formulations to evaluate the $N_{cr}$–$M_{cr}$ domain are now-adays available in literature: in particular, Trahair and Woolcock [52] considered the effects of combined uniform bending and axial load for stability of doubly-symmetric I beam–column elements, which were considered also by Machado [53] in the analysis of thin-walled composite beams. Mohri et al. [54] focused their atten-tion on the buckling of non-symmetric beam–columns and pro-posed closed formulas for I cross-sections under uniform loads. In Appendix A, an approach strictly deriving from these studies is proposed to evaluate the critical bending moment of beam–columns, reducing the critical lateral moment of the beam for the presence of axial load, which should be proposed in the steel design codes, allowing to reproduce more accurately the $N_{cr}$–$M_{cr}$ domain.

In the following, the theoretical approach summarized in Appendix A has been used in conjunction with appropriate FE

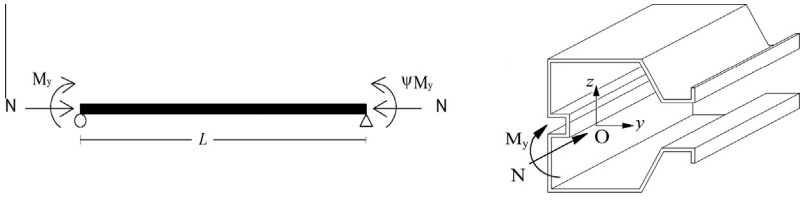


**Fig. 5.** The isolated member under gradient moment considered in the present study.

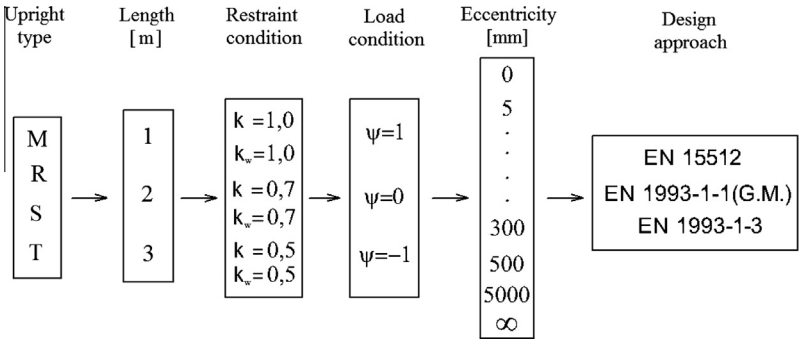


**Fig. 6.** Synopsis of the considered cases.

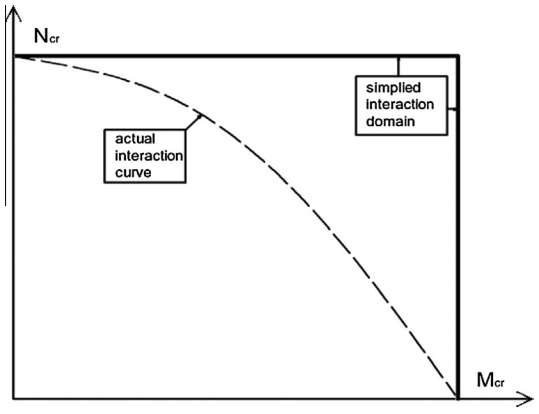


**Fig. 7.** Actual and simplified interaction buckling domain for beam–column.

simulations, because of the need to avoid any discussions about the availability of reliable values of the $C$ coefficients. Members with mono-symmetric or complex (asymmetric or non-symmetric) cross-section, or complete structures realized with them, should be accurately investigated via FE shell models: as an example, San-gle et al. [55] and Bajoria et al. [56] carried out extensive numerical researches on pallet racks via very refined finite element models using shell elements to simulate uprights, beams and connections. This modeling technique is however not properly indicated for routine rack design. Long time for preparing the mesh and re-analysis of the output data is necessary for each loading case, resulting hence extremely expensive from the computational point of view and for the great efforts required by designers, especially when applied to very cheap products, such as the steel storage systems. The use of suitable beam FE elements instead of shell elements appears to be an efficient alternative to model complete rack systems as well as cladding racks: research outcomes are herein based on the analyses via the 7 DOFs beam element formulation implemented in Ś iva. As previously mentioned, the presence of the 7th DOF (warping $\theta$) is an essential pre-requisite to capture the coupling between flexural and torsional buckling modes and Fig. 8 presents some typical buckling deformed shapes obtained from the eigenvalue analysis for each of the four considered cross-sections. It should be noted that the implemented formulation allows reproducing accurately the flexural–torsional buckling mode, which for open thin-walled cross section is usually characterized by a non-negligible distortion of the cross-section shape.

It is worth to mention that this model does not consider plasticity and large displacement and buckling loads are obtained via eigenvalue buckling analysis. As an example of the accuracy of the Śiva results, Table 2 can be considered, where the values of the critical load multiplier obtained via the theoretical approaches ($\alpha_{cr}^{Th}$) of columns and the lateral buckling moment of beams (see Appendix A for the associated equations) are reported over the corresponding value obtained by Śiva ($\alpha_{cr}^{Siva}$). In addition, the free software LTBeam [57,58] developed by CTICM, has been used to evaluate the critical load multiplier ($\alpha_{cr}^{LTBeam}$) and also the $\alpha_{cr}^{Th}/\alpha_{cr}^{LTBeam}$ ratio is reported between brackets in the same table. It can be noted that:

- generally, $\alpha_{cr}^{Th}/\alpha_{cr}^{Siva}$ and $\alpha_{cr}^{Th}/\alpha_{cr}^{LTBeam}$ ratios are quite similar to each other, confirming the good accuracy of the 7 DOFs FE beam formulation implemented in Śiva;
- in several cases, both $\alpha_{cr}^{Th}/\alpha_{cr}^{Siva}$ and $\alpha_{cr}^{Th}/\alpha_{cr}^{LTBeam}$ ratios are slightly different from unity, confirming the need of further research work to better calibrate the $C_1$ coefficient proposed in the code;
- in a very limited number of cases quite small differences can be noted between $\alpha_{cr}^{Siva}$ and $\alpha_{cr}^{Th}$ or $\alpha_{cr}^{LTBeam}$, especially for lower values of $k_w$. The difference from unity of $\alpha_{cr}^{Th}/\alpha_{cr}^{LTBeam}$ ratio is however limited, never greater than 15% with a mean value of the ratios presented in the table is 1.015.

Furthermore, the mutual influence between axial load and lateral bending moment for the buckling of the beam–column can be appraised by Fig. 9, related to the cases of restraint coefficients $k$ = $k_w$ = 1: both the domains obtained by Ś iva and the theoretical approach of part A3) of Appendix A, are presented, which are associated with a solid and dashed line, respectively. The buckling interaction domains are reported with reference to the critical axial load $n_{cr}$ and to the lateral buckling moment $m_{cr}$, both defined in non-dimensional form as:

$$n_{cr}(M) = \frac{N_{cr}(M)}{N_{cr}(M=0)} \tag{2a}$$

$$m_{cr}(M) = \frac{M_{cr}(N)}{M_{cr}(N=0;\psi=1)} \tag{2b}$$

Furthermore, it should be noted that the curves associated with different considered beam slenderness coincide practically with each other in the non-dimensional domain $n_{cr}$–$m_{cr}$. No great differences between FE and theoretical results can be observed and these seem mainly due to the $C_1$ values adopted to predict theoretically the buckling moment: the values between the brackets represent the $C_1$ coefficient arising directly from the FE analysis, mean values of which are 1.89 ($\psi$ = 0) and 2.72 ($\psi$ = −1). These values are quite similar to those proposed in Ref. [51], which recommends $C_1$ = 1.879 and $C_1$ = 2.752 for ($\psi$ = 0) and ($\psi$ = −1), respectively, but quite different from the values of 1.77 ($\psi$ = 0) and 2.60 ($\psi$ = −1) recommended from recent research calibration studies [59].

As to the other considered restraint conditions, i.e. $k$ = $k_w$ = 0.5 or $k$ = $k_w$ = 0.7, it is worth to mention that the associated domains are very similar to those plotted in Fig. 9 and the same comments

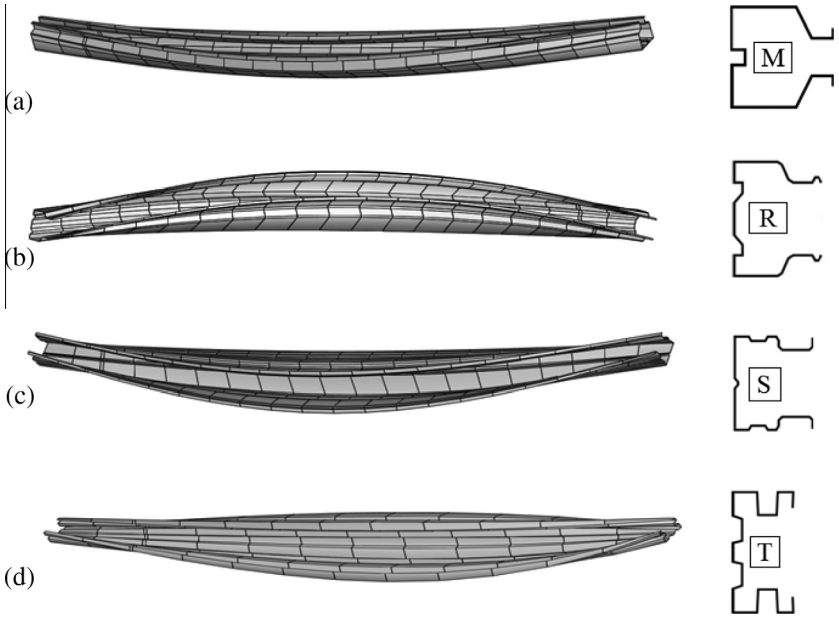


**Fig. 8.** Typical buckling shapes under axial load for the considered uprights, having member length equal to 2.0 m (Śiva graphical output).

**Table 2**
Prediction of the theoretical critical load multiplier via Śiva software (ratio $\frac{\alpha_{cr}^{th}}{\alpha_{cr}^{Siva}}$ in top position) and via LTBeam software (ratio $\frac{\alpha_{cr}^{LTbeam}}{\alpha_{cr}^{Siva}}$ in bottom position, between brackets).

| Ecc. | $\psi$ | Restraint conditions | *M* | | | *R* | | | *S* | | | *T* | | |
|---|---|---|---|---|---|---|---|---|---|---|---|---|---|---|
| | | | *L* = 1 m | *L* = 2 m | *L* = 3 m | *L* = 1 m | *L* = 2 m | *L* = 3 m | *L* = 1 m | *L* = 2 m | *L* = 3 m | *L* = 1 m | *L* = 2 m | *L* = 3 m |
| 0 | – | – | 1.000 (n.a.) | 0.999 (n.a.) | 0.998 (n.a.) | 1.000 (n.a.) | 1.000 (n.a.) | 1.000 (n.a.) | 0.999 (n.a.) | 1.000 (n.a.) | 1.000 (n.a.) | 0.999 (n.a.) | 1.001 (n.a.) | 1.000 (n.a.) |
| ∞ | $\psi = 1$ | $k_w = 1.0$ | 1.044 (1.048) | 1.060 (1.059) | 1.056 (1.052) | 1.027 (1.027) | 1.042 (1.042) | 1.008 (1.009) | 1.030 (1.029) | 1.013 (1.010) | 1.043 (1.037) | 1.052 (1.053) | 1.065 (1.068) | 1.063 (1.066) |
| | | $k_w = 0.7$ | 0.990 (1.000) | 0.988 (1.060) | 0.993 (1.064) | 0.954 (1.043) | 0.980 (1.072) | 0.985 (1.078) | 0.965 (1.055) | 0.933 (1.018) | 0.982 (1.071) | 0.965 (1.055) | 0.923 (1.009) | 0.992 (1.063) |
| | | $k_w = 0.5$ | 0.977 (1.072) | 0.977 (1.077) | 0.985 (1.059) | 0.977 (1.072) | 0.904 (1.020) | 0.978 (1.072) | 0.977 (1.081) | 0.978 (1.071) | 0.978 (1.052) | 0.881 (0.998) | 0.985 (1.016) | 0.993 (1.014) |
| | $\psi = 0$ | $k_w = 1.0$ | 1.032 (1.018) | 1.039 (1.025) | 1.072 (1.055) | 1.007 (0.994) | 1.068 (1.056) | 1.047 (1.034) | 1.031 (1.017) | 1.054 (1.037) | 1.079 (1.057) | 1.024 (1.012) | 1.065 (1.052) | 1.034 (1.020) |
| | | $k_w = 0.7$ | 1.064 (1.033) | 1.164 (1.034) | 1.106 (0.963) | 1.218 (1.061) | 1.093 (1.062) | 1.189 (1.038) | 1.107 (0.992) | 1.089 (1.055) | 1.089 (1.016) | 1.079 (1.048) | 1.054 (1.025) | 1.059 (1.030) |
| | | $k_w = 0.5$ | 1.123 (1.080) | 1.123 (1.080) | 1.123 (1.069) | (1.105) (1.035) | (1.053) (1.041) | (1.105) (1.091) | (1.011) (1.004) | (1.103) (1.090) | (1.017) (1.002) | 1.122 (1.061) | 1.131 (1.018) | 1.043) (1.030) |
| | $\psi = -1$ | $k_w = 1.0$ | 1.076 (1.072) | 1.082 (1.077) | 1.068 (1.059) | 1.079 (1.075) | 1.032 (1.029) | 1.062 (1.059) | 1.017 (1.012) | 1.059 (1.052) | 1.047 (1.036) | 1.055 (1.052) | 1.078 (1.076) | 1.095 (1.091) |
| | | $k_w = 0.7$ | 1.014 (1.003) | 1.018 (0.997) | 1.025 (1.011) | 1.011 (0.983) | 0.900 (0.990) | 1.010 (0.999) | 1.011 (0.999) | 1.011 (0.997) | 0.999 (0.976) | 1.006 (0.998) | 0.909 (0.999) | 0.911 (1.001) |
| | | $k_w = 0.5$ | 0.853 (1.004) | 0.849 (1.004) | 0.879 (1.013) | 0.848 (0.994) | 0.847 (1.002) | 0.925 (1.002) | 0.896 (1.004) | 0.850 (1.003) | 0.853 (1.002) | 0.849 (1.004) | 0.851 (1.004) | 0.895 (1.004) |

already proposed maintain their validity. Also with reference to these data, not herein directly reported, the differences between the Śiva and the theoretical values are slightly greater, but never greater than 15% (in case of higher eccentricity), confirming the need of further investigation on $C_1$ coefficient.

## 4. Upright design in accordance with EN 15512

European rack design is usually carried out on basis of EN 15512 rack Provisions [5], that is a guidance containing the principles for racks monotonic design but it represents, at the same time, the reference for the verification of members subjected to seismic loading. Very important indications are given in the code for what concerns the rack features and the design assisted by testing, despite the fact that, as already declared, further important investigations are urgently required. As to the verification checks, attention is herein focused on the vertical elements of the racks modeled as planar frames and hence uprights are subjected to axial load $N_{Ed}$ and bending moment about the principal (symmetry) cross-section axis, $M_{y,Ed}$. Owing to the use of open thin-walled cross-sections, uprights are usually interested by lateral–torsional buckling and, with reference to stability checks, the following condition has to be fulfilled:

$$\left(\frac{N_{Ed}}{\chi_{\min} A_{eff} f_y/\gamma_M}\right) + \left(\frac{k_{LT} M_{y,Ed}}{\chi_{LT} W_{eff,y} f_y/\gamma_M}\right) = (n) + (m_y) \leqslant 1 \tag{3}$$

in which $\chi$ is the reduction factor accounting for buckling phenomena, $A$ and $W$ are the area and the cross-section modulus, respectively, $f_y$ is the material yielding strength and subscript *eff* indicates the use of the effective cross section properties, when different from the gross ones (not in these cases).

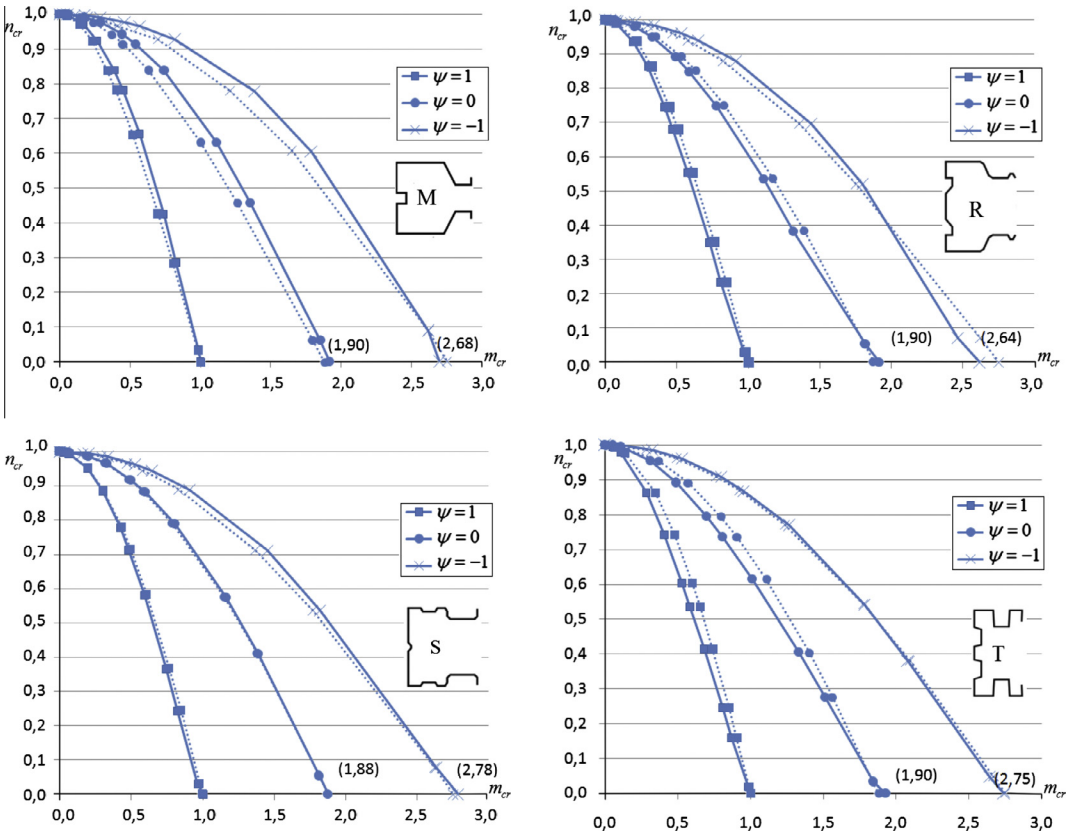


**Fig. 9.** Non-dimensional buckling interaction domains obtained by means of Śiva FE program (solid line) and Eq. (A8) (dashed line).

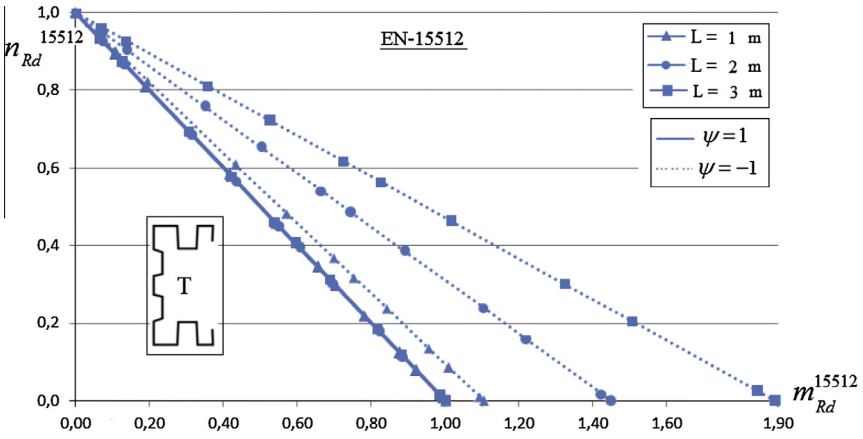


**Fig. 10.** T_uprights: non dimensional beam–column domains $n_{Rd}^{15512}$–$m_{Rd}^{15512}$ in accordance with EN 15512.

In Eq. (3), first term ($n$) is associated with the effect of the axial load and the second one ($m_y$) is related to the bending moment contribution.

For class 3 profiles ($A = A_{eff}$), the evaluation of the relative slenderness $\bar{\lambda}$ for axial load is at first required, which is defined as:

$$\bar{\lambda} = \sqrt{\frac{A \cdot f_y}{N_{cr}}} = \sqrt{\frac{A_{eff} \cdot f_y}{N_{cr}}} \tag{4}$$

in which $N_{cr}$ is the elastic critical load for the appropriate buckling mode: flexural ($N_{cr,y}$ and $N_{cr,z}$), torsional ($N_{cr,T}$), or flexural–torsional ($N_{cr,FT}$), the equations which are defined in the Appendix A. Owing to the need of reducing the number of parameters influencing the research outcomes, distortional buckling has been assumed not relevant for design purposes. Term $\chi_{\min}$ depends strictly on the maximum value of the relative slenderness $\bar{\lambda}$, being defined as:

$$\chi = \frac{1}{\phi + \sqrt{\phi^2 - \bar{\lambda}^2}} \leqslant 1 \tag{5a}$$

where $\phi$ is defined:

$$\phi = 0.5\lfloor 1 + 0.34(\bar{\lambda} - 0.2) + \bar{\lambda}^2 \rfloor \tag{5b}$$

As to the contribution due to bending moment about the principal major axis ($m_y$), the reduction factor for lateral-torsional buckling ($\chi_{LT}$) can be determined via expression (4) substituting the relative

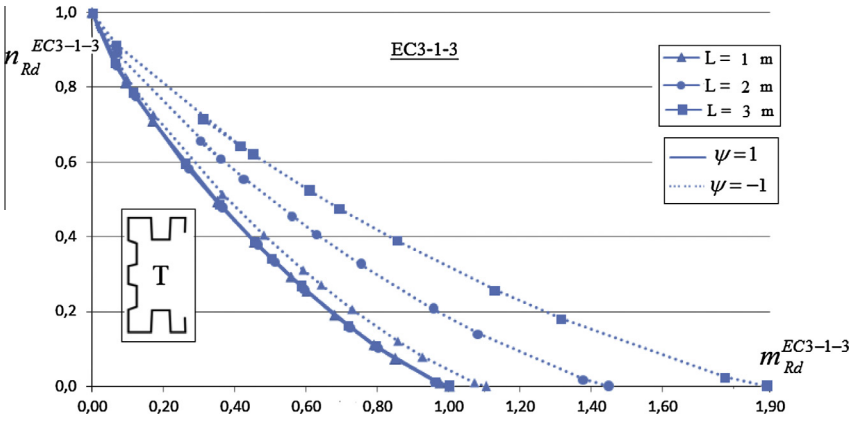


**Fig. 11.** T_uprights: non dimensional beam–column domains $n_{Rd}^{EC3\text{-}1\text{-}3}$–$m_{Rd}^{EC3\text{-}1\text{-}3}$ in accordance with EC3-1-3.

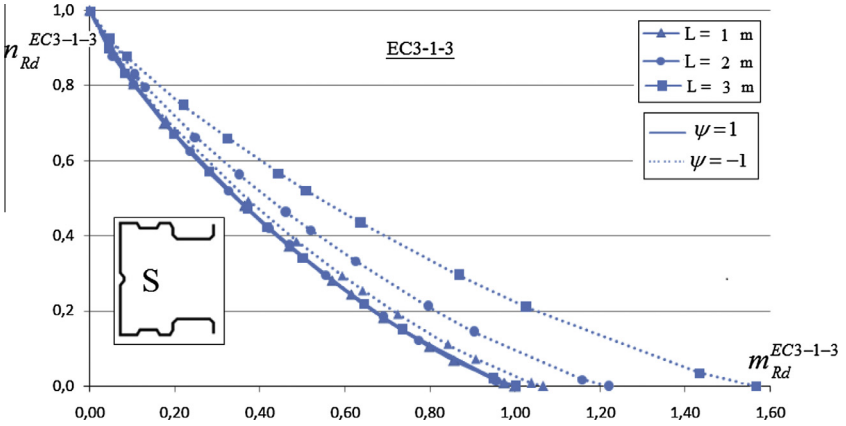


**Fig. 12.** S_uprights: non dimensional beam–column domains $n_{Rd}^{EC3\text{-}1\text{-}3}$–$m_{Rd}^{EC3\text{-}1\text{-}3}$ in accordance with EC3-1-3.

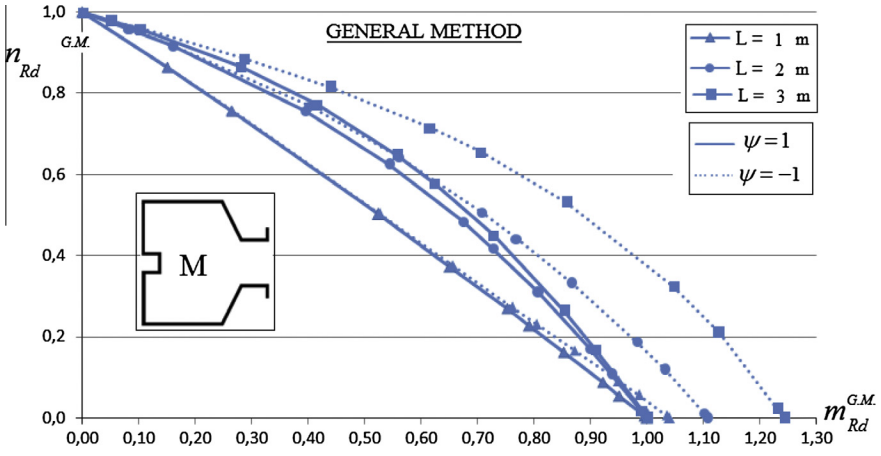


**Fig. 13.** M_uprights: non dimensional beam–column domains $n_{Rd}^{G.M.}$–$m_{Rd}^{G.M.}$ in accordance with EC3-1-1.

slenderness for axial load ($\bar{\lambda}$) with the one for lateral–torsional buckling of beam ($\bar{\lambda}_{LT}$) defined as:

$$\bar{\lambda}_{LT} = \sqrt{\frac{W_{eff,y} f_y}{M_{cr}}} \tag{6}$$

where term $M_{cr}$ is the elastic critical moment for lateral–torsional buckling (Appendix A).

Term $k_{LT}$ is defined as:

$$k_{LT} = 1 - \frac{\mu_{LT} N_{Ed}}{\chi_z A_{eff} f_y} \leqslant 1 \tag{7}$$

with $\mu_{LT}$ defined as:

$$\mu_{LT} = 0.15 \cdot (\bar{\lambda}_z \beta_{M,LT} - 1) \leqslant 0.9 \tag{8}$$

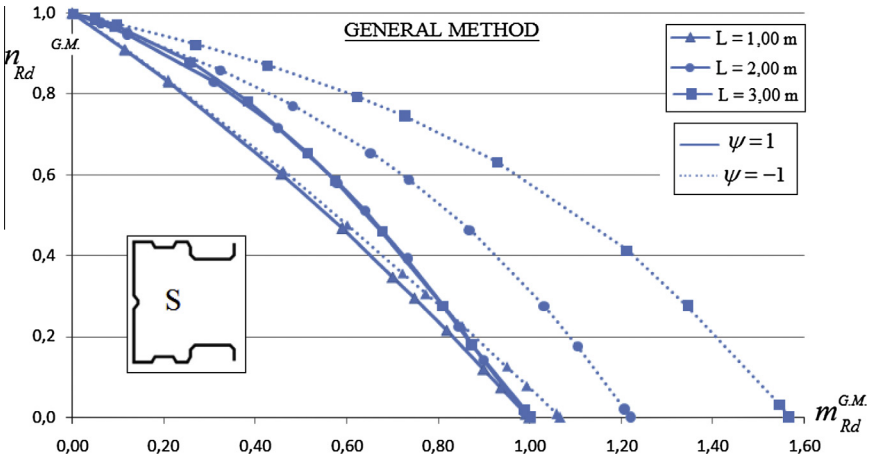


**Fig. 14.** S_uprights: non dimensional beam–column domains $n_{Rd}^{G.M.}$–$m_{Rd}^{G.M.}$ in accordance with EC3-1-1.

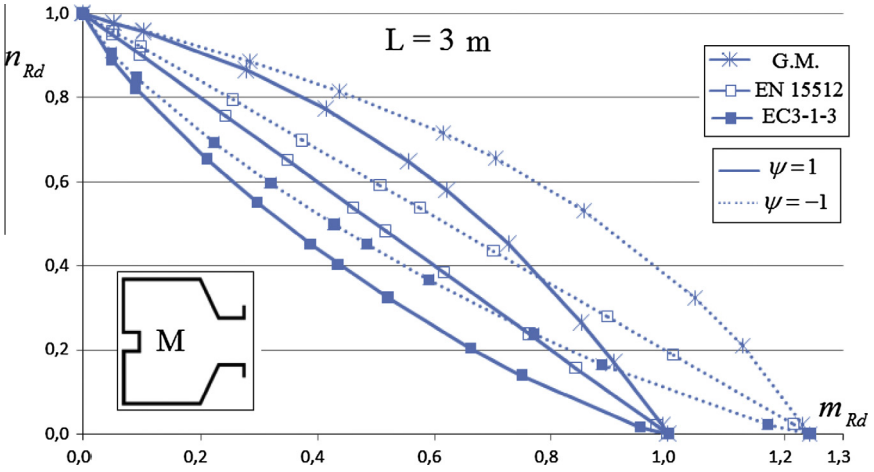


**Fig. 15.** M_uprights: direct comparison between the beam–column dimensionless $n_{Rd}$–$m_{Rd}$ domains in accordance with the considered design approaches.

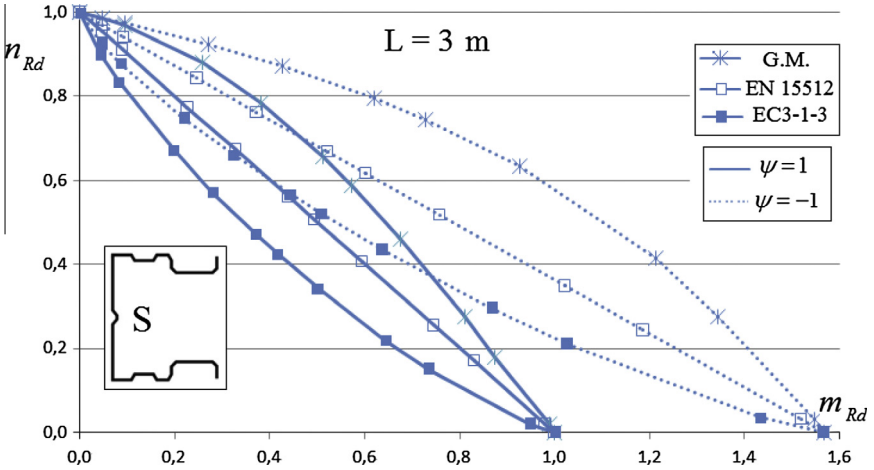


**Fig. 16.** S_uprights: direct comparison between the beam–column dimensionless $n_{Rd}$–$m_{Rd}$ domains in accordance with the considered design approaches.

where $\bar{\lambda}_z$ is the slenderness ratio for flexural buckling and $\beta_{M,LT}$ is an equivalent uniform moment factor for lateral–torsional buckling, which, in case of bending moment with a linear variation between the critical points of the uprights, is defined as:

$$\beta_{M,LT} = 1.8 - 0.7\frac{M_{\min}}{M_{\max}} \tag{9}$$

where $M_{\min}$ and $M_{\max}$ indicate respectively the minimum and the maximum bending moment at the ends of the element.

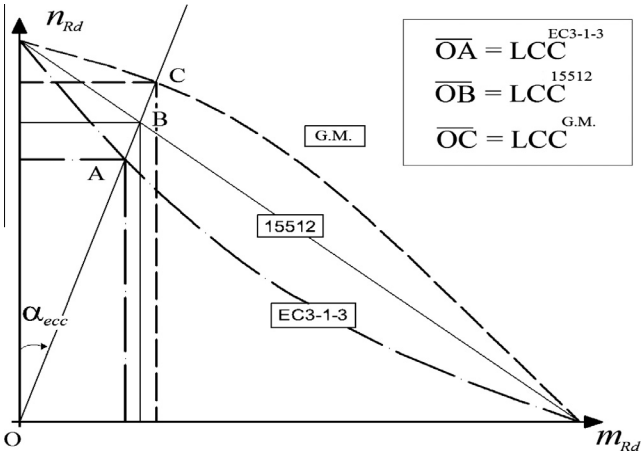


**Fig. 17.** Definition of the load carrying capacity ($LCC^L$) for the generic value of the eccentricity angle $\alpha_{ecc}$.

It should be noted that this design approach was already proposed in the previous version (ENV version) of EC3 [51] but it has been removed approximately ten years ago for the update EN version [45] due to its inaccuracy not only for doubly symmet-ric cross-section beam–columns but also for members having mono-symmetric cross-section as well as for rack components. To this purpose, it is worth to mention that in the general case of beam–column subjected to the bending moment $M_z$, in addition to the one $M_y$ considered in the following, four different effective cross-sections have to be evaluated: one for the sole axial load, one for the sole bending moment about symmetry axis and two for the sole bending moment about non-symmetry principal axis. The interaction between axial force and bending moment is hence neglected, which influences significantly the effective cross-section properties, as demonstrated in [60,61]. Furthermore, no practical indications are given to designers for what concerns the buckling interaction between compression and flexure. In routine design this well-established interaction is usually neglected: as previously shown (Fig. 7) the reduction factors contained in the beam–column verification Eq. (3) are evaluated with reference to the case of the sole axial load ($\chi_{min}$) and to the case of the sole bending moment ($\chi_{LT}$) and are totally independent from the value of the axial load eccentricity.

### 4.1. Numerical applications

For all the considered cases (Fig. 6), EN 15512 code was applied in order to evaluate the load carrying capacity in terms of axial load ($N_{Rd}^{15512}$) and bending resistance ($M_{y,Rd}^{15512} = N_{Rd}^{15512} \cdot e$). The equation associated with this approach leads to linear $N_{Rd}^{15512} - M_{y,Rd}^{15512}$ domain, depending only on geometrical and mechanical properties, being the value of $\chi$ and $\chi_{LT}$ constant for each case independent from the axial load eccentricity. As an example, Fig. 10 can be considered where the domains for $\psi = 1$ and $\psi = -1$ are proposed for the T_uprights when $k = k_w = 1$. The cases associated with $\psi = 0$ have not been plotted, being approximately in the middle of the others. These domains are presented in the non-dimensional form $n_{Rd}$–$m_{Rd}$, being $n_{Rd}^{15512} = \frac{N_{Rd}^{15512}}{N_{Rd}^{15512}(M=0)}$ and $m_{Rd}^{15512} = \frac{M_{y,Rd}^{15512}(N)}{M_{y,Rd}^{15512}(N=0;\psi=1)}$. It should be noted that, for non-uniform moment distributions by increasing the beam length the surface of safe region increases too, owing to the most favorable load condition (gradient moment distribution) with respect to the uniform one on the verification buckling checks.

## 5. Upright design in accordance with EN 1993-1-3

As alternative, reference can be made to the design approach typically proposed for cold-formed thin-walled beam–column subjected to mono-axial bending (in the following indicated as EC3-1-3). In part 1-3 of EC3 [40] the following equation has to be fulfilled:

$$\left(\frac{N_{Ed}}{N_{Rd}}\right)^{0.8} + \left(\frac{M_{y,Ed}}{M_{y,Rd}}\right)^{0.8} = (n)^{0.8} + \left(\frac{m_y}{k_{LT}}\right)^{0.8} \leqslant 1 \qquad (10)$$

**Table 3**
Values of the $\frac{LCC^{15512}}{LCC^{EC3\text{-}1\text{-}3}}$ ratio when $k = k_w = 1$.

| $e$ [mm] | $\psi$ | $L$ = 1 m | | | | $L$ = 2 m | | | | $L$ = 3 m | | | |
|---|---|---|---|---|---|---|---|---|---|---|---|---|---|
| | | $M$ | $R$ | $S$ | $T$ | $M$ | $R$ | $S$ | $T$ | $M$ | $R$ | $S$ | $T$ |
| 5 | $\psi = 1$ | 1.122 | 1.101 | 1.105 | 1.101 | 1.086 | 1.084 | 1.071 | 1.080 | 1.065 | 1.067 | 1.061 | 1.078 |
| | $\psi = 0$ | 1.121 | 1.100 | 1.102 | 1.098 | 1.082 | 1.080 | 1.065 | 1.068 | 1.059 | 1.061 | 1.050 | 1.059 |
| | $\psi = -1$ | 1.120 | 1.099 | 1.101 | 1.096 | 1.081 | 1.079 | 1.194 | 1.064 | 1.057 | 1.059 | 1.046 | 1.053 |
| 10 | $\psi = 1$ | 1.160 | 1.139 | 1.143 | 1.140 | 1.122 | 1.120 | 1.115 | 1.115 | 1.096 | 1.100 | 1.091 | 1.113 |
| | $\psi = 0$ | 1.159 | 1.138 | 1.141 | 1.136 | 1.118 | 1.116 | 1.096 | 1.100 | 1.088 | 1.091 | 1.077 | 1.088 |
| | $\psi = -1$ | 1.158 | 1.137 | 1.139 | 1.134 | 1.117 | 1.114 | 1.094 | 1.481 | 1.086 | 1.089 | 1.071 | 1.443 |
| 50 | $\psi = 1$ | 1.180 | 1.188 | 1.188 | 1.188 | 1.189 | 1.188 | 1.183 | 1.187 | 1.178 | 1.180 | 1.175 | 1.186 |
| | $\psi = 0$ | 1.181 | 1.189 | 1.188 | 1.189 | 1.188 | 1.187 | 1.178 | 1.181 | 1.172 | 1.175 | 1.161 | 1.172 |
| | $\psi = -1$ | 1.181 | 1.189 | 1.188 | 1.189 | 1.187 | 1.187 | 1.176 | 1.178 | 1.170 | 1.172 | 1.154 | 1.165 |
| 100 | $\psi = 1$ | 1.150 | 1.169 | 1.166 | 1.169 | 1.180 | 1.182 | 1.188 | 1.184 | 1.189 | 1.189 | 1.189 | 1.185 |
| | $\psi = 0$ | 1.151 | 1.170 | 1.168 | 1.172 | 1.183 | 1.184 | 1.189 | 1.189 | 1.189 | 1.189 | 1.186 | 1.189 |
| | $\psi = -1$ | 1.152 | 1.171 | 1.169 | 1.173 | 1.183 | 1.184 | 1.189 | 1.189 | 1.189 | 1.189 | 1.183 | 1.187 |
| 150 | $\psi = 1$ | 1.127 | 1.149 | 1.146 | 1.149 | 1.165 | 1.182 | 1.178 | 1.170 | 1.183 | 1.181 | 1.185 | 1.172 |
| | $\psi = 0$ | 1.129 | 1.150 | 1.148 | 1.153 | 1.168 | 1.184 | 1.182 | 1.180 | 1.186 | 1.185 | 1.189 | 1.186 |
| | $\psi = -1$ | 1.130 | 1.151 | 1.149 | 1.154 | 1.169 | 1.184 | 1.184 | 1.183 | 1.187 | 1.186 | 1.189 | 1.189 |
| 500 | $\psi = 1$ | 1.067 | 1.084 | 1.081 | 1.084 | 1.100 | 1.102 | 1.118 | 1.106 | 1.126 | 1.122 | 1.131 | 1.109 |
| | $\psi = 0$ | 1.068 | 1.086 | 1.083 | 1.088 | 1.104 | 1.106 | 1.126 | 1.122 | 1.135 | 1.131 | 1.149 | 1.135 |
| | $\psi = -1$ | 1.069 | 1.086 | 1.084 | 1.089 | 1.105 | 1.108 | 1.129 | 1.127 | 1.138 | 1.135 | 1.156 | 1.144 |
| 5000 | $\psi = 1$ | 1.014 | 1.019 | 1.018 | 1.019 | 1.023 | 1.024 | 1.030 | 1.026 | 1.033 | 1.031 | 1.035 | 1.026 |
| | $\psi = 0$ | 1.015 | 1.019 | 1.019 | 1.020 | 1.025 | 1.025 | 1.033 | 1.031 | 1.036 | 1.035 | 1.043 | 1.036 |
| | $\psi = -1$ | 1.015 | 1.019 | 1.019 | 1.020 | 1.025 | 1.026 | 1.034 | 1.033 | 1.038 | 1.036 | 1.050 | 1.041 |

**Table 4**
Values of the $\frac{LCC^{G.M.}}{LCC^{15512}}$ ratio when $k = k_w = 1$.

| $e$ [mm] | $\psi$ | $L$ = 1 m | | | | $L$ = 2 m | | | | $L$ = 3 m | | | |
|---|---|---|---|---|---|---|---|---|---|---|---|---|---|
| | | $M$ | $R$ | $S$ | $T$ | $M$ | $R$ | $S$ | $T$ | $M$ | $R$ | $S$ | $T$ |
| 5 | $\psi = 1$ | 1.014 | 1.004 | 1.025 | 1.026 | 1.042 | 1.029 | 1.036 | 1.046 | 1.031 | 1.033 | 1.034 | 1.047 |
| | $\psi = 0$ | 1.010 | 1.002 | 1.020 | 1.021 | 1.036 | 1.023 | 1.029 | 1.033 | 1.024 | 1.026 | 1.022 | 1.029 |
| | $\psi = -1$ | 1.008 | 1.000 | 1.018 | 1.018 | 1.034 | 1.021 | 1.026 | 1.029 | 1.021 | 1.023 | 1.018 | 1.024 |
| 10 | $\psi = 1$ | 1.021 | 1.007 | 1.040 | 1.041 | 1.076 | 1.052 | 1.066 | 1.077 | 1.060 | 1.059 | 1.062 | 1.072 |
| | $\psi = 0$ | 1.014 | 1.002 | 1.033 | 1.034 | 1.066 | 1.042 | 1.055 | 1.059 | 1.047 | 1.048 | 1.041 | 1.050 |
| | $\psi = -1$ | 1.011 | 1.001 | 1.030 | 1.031 | 1.063 | 1.038 | 1.051 | 1.055 | 1.043 | 1.045 | 1.034 | 1.047 |
| 50 | $\psi = 1$ | 1.024 | 1.012 | 1.057 | 1.049 | 1.168 | 1.086 | 1.165 | 1.109 | 1.188 | 1.127 | 1.165 | 1.085 |
| | $\psi = 0$ | 1.012 | 1.004 | 1.047 | 1.049 | 1.156 | 1.084 | 1.170 | 1.135 | 1.176 | 1.141 | 1.152 | 1.096 |
| | $\psi = -1$ | 1.007 | 1.003 | 1.039 | 1.049 | 1.150 | 1.080 | 1.167 | 1.167 | 1.168 | 1.148 | 1.142 | 1.162 |
| 100 | $\psi = 1$ | 1.019 | 1.009 | 1.043 | 1.035 | 1.145 | 1.069 | 1.151 | 1.084 | 1.201 | 1.111 | 1.160 | 1.064 |
| | $\psi = 0$ | 1.009 | 1.003 | 1.037 | 1.037 | 1.140 | 1.074 | 1.183 | 1.124 | 1.220 | 1.150 | 1.198 | 1.084 |
| | $\psi = -1$ | 1.004 | 1.003 | 1.031 | 1.041 | 1.137 | 1.074 | 1.192 | 1.180 | 1.222 | 1.175 | 1.209 | 1.197 |
| 150 | $\psi = 1$ | 1.015 | 1.006 | 1.033 | 1.026 | 1.117 | 1.055 | 1.123 | 1.067 | 1.178 | 1.089 | 1.137 | 1.050 |
| | $\psi = 0$ | 1.008 | 1.002 | 1.030 | 1.029 | 1.116 | 1.061 | 1.183 | 1.105 | 1.210 | 1.134 | 1.191 | 1.068 |
| | $\psi = -1$ | 1.004 | 1.002 | 1.025 | 1.034 | 1.115 | 1.064 | 1.192 | 1.161 | 1.221 | 1.165 | 1.225 | 1.188 |
| 500 | $\psi = 1$ | 1.005 | 1.001 | 1.010 | 1.008 | 1.045 | 1.019 | 1.041 | 1.026 | 1.077 | 1.026 | 1.052 | 1.018 |
| | $\psi = 0$ | 1.004 | 1.000 | 1.012 | 1.010 | 1.046 | 1.025 | 1.071 | 1.043 | 1.103 | 1.059 | 1.104 | 1.017 |
| | $\psi = -1$ | 1.004 | 1.001 | 1.010 | 1.013 | 1.051 | 1.027 | 1.083 | 1.070 | 1.117 | 1.081 | 1.133 | 1.092 |
| 5000 | $\psi = 1$ | 1.001 | 1.000 | 1.000 | 1.001 | 1.006 | 1.001 | 1.000 | 0.998 | 1.010 | 0.991 | 1.009 | 1.001 |
| | $\psi = 0$ | 1.000 | 1.000 | 1.001 | 0.999 | 1.005 | 1.002 | 1.010 | 1.006 | 1.009 | 1.001 | 1.008 | 0.997 |
| | $\psi = -1$ | 1.001 | 1.000 | 1.001 | 1.001 | 1.007 | 1.003 | 1.011 | 1.009 | 1.013 | 1.010 | 1.019 | 1.015 |

where $N_{Rd}$ is the design buckling resistance of a compression member according to the criteria based on the actual buckling mode, i.e. the minimum between flexural, torsional and torsional–flexural buckling) and $M_{y,Rd}$ is the design bending moment resistance.

Both $N_{Rd}$ and $M_{y,Rd}$ have been evaluated by the same equations recommended in EN 15512: the only difference from Eq. (3) is the presence of the exponent 0.8 and the absence of term $k_{LT}$ in the $m_y$ contribution. The weak points associated with the previous method can be totally extended also to this one.

### 5.1. Numerical applications

For all the considered cases this method was also applied to evaluate the load carrying capacity in terms of axial load ($N_{Rd}^{EC3\text{-}1\text{-}3}$) and bending resistance ($M_{y,Rd}^{EC3\text{-}1\text{-}3} = N_{Rd}^{EC3\text{-}1\text{-}3} \cdot e$). As for the EN 15512 approach, the dimensionless $n_{Rd}$–$m_{Rd}$ domains can be considered, defining $n_{Rd}^{EC3\text{-}1\text{-}3} = \frac{N_{Rd}^{EC3\text{-}1\text{-}3}}{N_{Rd}^{EC3\text{-}1\text{-}3}(M=0)}$ and $m_{Rd}^{EC3\text{-}1\text{-}3} = \frac{M_{Rd}^{EC3\text{-}1\text{-}3}(N)}{M_{y,Rd}^{EC3\text{-}1\text{-}3}(N=0;\psi=1)}$. Owing to the presence of an exponent lower than

**Table 5**
Values of the $\frac{LCC^{G.M.}}{LCC^{EC3\text{-}1\text{-}3}}$ ratio when $k = k_w = 1$.

| $e$ [mm] | $\psi$ | $L$ = 1 m | | | | $L$ = 2 m | | | | $L$ = 3 m | | | |
|---|---|---|---|---|---|---|---|---|---|---|---|---|---|
| | | $M$ | $R$ | $S$ | $T$ | $M$ | $R$ | $S$ | $T$ | $M$ | $R$ | $S$ | $T$ |
| 5 | $\psi = 1$ | 1.138 | 1.106 | 1.132 | 1.130 | 1.131 | 1.115 | 1.109 | 1.130 | 1.098 | 1.102 | 1.097 | 1.128 |
| | $\psi = 0$ | 1.132 | 1.101 | 1.125 | 1.120 | 1.121 | 1.106 | 1.096 | 1.103 | 1.084 | 1.089 | 1.073 | 1.089 |
| | $\psi = -1$ | 1.130 | 1.100 | 1.121 | 1.116 | 1.118 | 1.102 | 0.922 | 1.095 | 1.079 | 1.083 | 1.064 | 1.078 |
| 10 | $\psi = 1$ | 1.184 | 1.148 | 1.189 | 1.186 | 1.207 | 1.179 | 1.177 | 1.201 | 1.162 | 1.164 | 1.159 | 1.193 |
| | $\psi = 0$ | 1.175 | 1.141 | 1.178 | 1.174 | 1.192 | 1.162 | 1.156 | 1.166 | 1.140 | 1.144 | 1.121 | 1.143 |
| | $\psi = -1$ | 1.171 | 1.138 | 1.173 | 1.200 | 1.187 | 1.156 | 0.982 | 1.210 | 1.132 | 1.137 | 1.107 | 1.230 |
| 50 | $\psi = 1$ | 1.209 | 1.202 | 1.255 | 1.247 | 1.388 | 1.290 | 1.377 | 1.317 | 1.400 | 1.330 | 1.369 | 1.287 |
| | $\psi = 0$ | 1.196 | 1.193 | 1.244 | 1.247 | 1.373 | 1.287 | 1.378 | 1.340 | 1.378 | 1.341 | 1.337 | 1.285 |
| | $\psi = -1$ | 1.189 | 1.190 | 1.235 | 1.247 | 1.365 | 1.282 | 1.227 | 1.374 | 1.367 | 1.346 | 1.319 | 1.354 |
| 100 | $\psi = 1$ | 1.172 | 1.179 | 1.216 | 1.210 | 1.352 | 1.264 | 1.367 | 1.284 | 1.428 | 1.320 | 1.380 | 1.261 |
| | $\psi = 0$ | 1.162 | 1.174 | 1.212 | 1.215 | 1.348 | 1.271 | 1.407 | 1.336 | 1.450 | 1.368 | 1.420 | 1.289 |
| | $\psi = -1$ | 1.157 | 1.173 | 1.205 | 1.221 | 1.345 | 1.272 | 1.296 | 1.403 | 1.453 | 1.397 | 1.430 | 1.421 |
| 150 | $\psi = 1$ | 1.144 | 1.156 | 1.183 | 1.179 | 1.301 | 1.230 | 1.323 | 1.248 | 1.393 | 1.286 | 1.347 | 1.231 |
| | $\psi = 0$ | 1.138 | 1.153 | 1.183 | 1.186 | 1.303 | 1.241 | 1.375 | 1.304 | 1.436 | 1.344 | 1.416 | 1.267 |
| | $\psi = -1$ | 1.134 | 1.154 | 1.178 | 1.193 | 1.303 | 1.245 | 1.291 | 1.373 | 1.450 | 1.382 | 1.456 | 1.412 |
| 500 | $\psi = 1$ | 1.073 | 1.086 | 1.093 | 1.093 | 1.149 | 1.123 | 1.163 | 1.136 | 1.213 | 1.152 | 1.190 | 1.129 |
| | $\psi = 0$ | 1.073 | 1.085 | 1.097 | 1.098 | 1.154 | 1.133 | 1.206 | 1.169 | 1.252 | 1.198 | 1.268 | 1.155 |
| | $\psi = -1$ | 1.073 | 1.089 | 1.096 | 1.104 | 1.161 | 1.138 | 1.165 | 1.205 | 1.271 | 1.226 | 1.310 | 1.250 |
| 5000 | $\psi = 1$ | 1.015 | 1.019 | 1.018 | 1.020 | 1.029 | 1.026 | 1.030 | 1.024 | 1.043 | 1.022 | 1.044 | 1.028 |
| | $\psi = 0$ | 1.015 | 1.019 | 1.020 | 1.019 | 1.030 | 1.027 | 1.043 | 1.037 | 1.046 | 1.036 | 1.052 | 1.034 |
| | $\psi = -1$ | 1.015 | 1.019 | 1.020 | 1.021 | 1.032 | 1.029 | 1.014 | 1.042 | 1.051 | 1.046 | 1.050 | 1.057 |

unity in Eq. (10), these domains are all convex, which are presented as examples in Fig. 11 (T_uprights) and Fig. 12 (S_uprights) for $k = k_w = 1$. When $\psi = 1$, they coincide for the three different consid-ered values of the length, owing to the criteria followed to present the dimensionless domains. Also in this case by increasing the beam length, the benefits due to non-uniform bending distribution increase and amplitude of the safe region increase too.

## 6. Upright design in accordance with EN 1993-1-1

Eurocode 3 in its general part 1-1 [45] proposes a quite innovative and interesting [62–64] design approach, the so-called General Method (in the following indicated as G.M.), for the stability design of structural components having geometrical, loading or supporting irregularity. In particular, this method [58–60] allows to assess the lateral and the lateral–torsional buckling resistance of steel components under compression and mono-axial bending in the plane. Overall resistance to out-of-plane buckling for frames as well as for isolated members is verified when:

$$\frac{\chi_{op}\alpha_{ult.k}}{\gamma_{M1}} \geqslant 1 \tag{11}$$

where $\alpha_{ult,k}$ is the minimum load amplifier to reach characteristic resistance, without lateral and torsional buckling into account, and $\chi_{op}$ is the reduction factor for lateral and lateral torsional buckling.

For the considered cases, upright cross-sections in class 3 guarantee that plastic hinges do not form in members because rack collapse is generally due to interaction between upright instability and plasticity in the beam-to-column joints as well as in the base-plate connections, as also confirmed by an experimental research which includes several full scale push-over rack tests [65].

As a consequence, ultimate load multiplier for cross-section resistance, $\alpha_{ult,k}$ can be obtained as:

$$\frac{1}{\alpha_{ult,k}} = \frac{N_{Ed}}{N_{Rk}} + \frac{M_{y,Ed}}{M_{y,Rk}} \tag{12}$$

where $N_{Rk}$ and $M_{y,Rk}$ are the squash load and the first yielding (elastic) moment, respectively, being the cross-sections in class 3.

By using Eq. (11), term $\chi_{op}$ is evaluated on the basis of the value of the global relative slenderness $\bar{\lambda}_{op}$ defined as:

$$\bar{\lambda}_{op} = \sqrt{\frac{\alpha_{ult.k}}{\alpha_{cr,op}}} \tag{13}$$

where $\alpha_{cr,op}$ is the minimum buckling multiplier for the in plane design loads.

Reduction factor $\chi_{op}$ for the overall buckling phenomena, strictly depending on the geometry as well as on the load condition (axial load–bending moment interaction) has to be evaluated in accordance with Eq. (5). For each value of the considered eccentricity $e$, the axial member resistance $N_{Rd}^{G.M.}$ and the associated bending resistance $M_{Rd}^{G.M.}$ have been determined as:

$$N_{Rd}^{G.M.} = \frac{\chi_{op} \cdot f_y}{\frac{1}{A} + \frac{e}{W_y}} \tag{14a}$$

$$M_{Rd}^{G.M.} = N_{Rd}^{G.M.} \cdot e \tag{14b}$$

### 6.1. Numerical applications

The General Method presented in EC3-1-1 was applied to all the considered cases to obtain dimensionless $n_{Rd}$–$m_{Rd}$ domains, defining $n_{Rd}^{G.M.} = \frac{N_{Rd}^{G.M.}}{N_{Rd}^{G.M.}(M=0)}$ and $m_{Rd}^{G.M.} = \frac{M_{Rd}^{G.M.}(N)}{M_{Rd}^{G.M.}(N=0;\psi=0)}$. Buckling analyses via Śiva software have been executed by modeling beam–column cases via a refined mesh (15 beam elements) with 7 DOFs beam

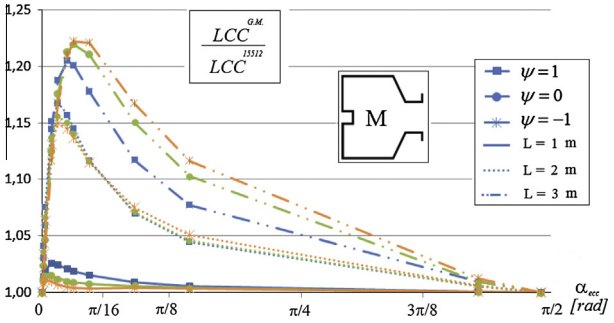


**Fig. 18.** $\frac{LCC^{G.M.}}{LCC^{15512}} - \alpha_{ecc}$ relationships for the M_uprigths.

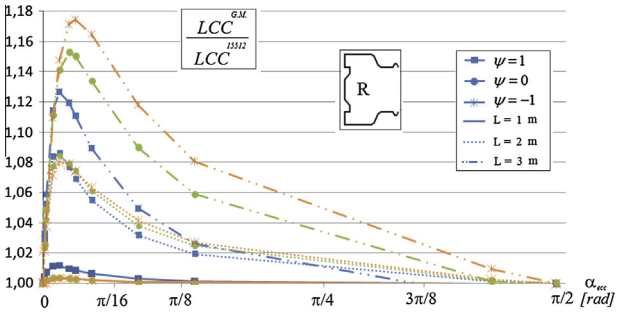


**Fig. 19.** $\frac{LCC^{G.M.}}{LCC^{15512}} - \alpha_{ecc}$ relationships for the R_uprigths.

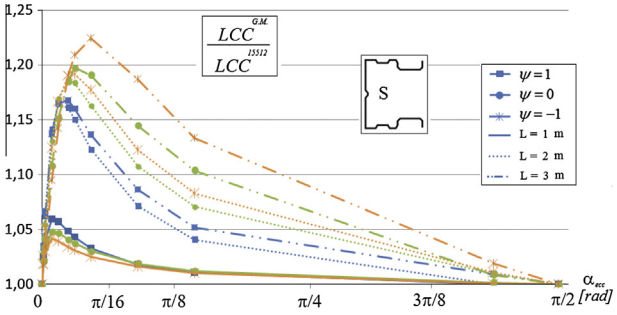


**Fig. 20.** $\frac{LCC^{G.M.}}{LCC^{15512}} - \alpha_{ecc}$ relationships for the S_uprigths.

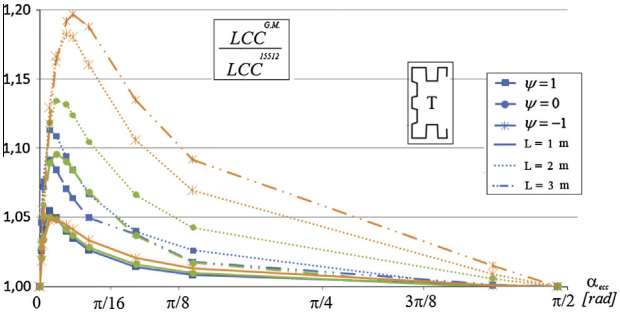


**Fig. 21.** $\frac{LCC^{G.M.}}{LCC^{15512}} - \alpha_{ecc}$ relationships for the T_uprigths.

FE elements. Suitable end restraints allow for the simulation of different rotation and warping restraints, directly accounted via $k$ and $k_w$ coefficients, respectively, in the other approaches. These domains are practically linear for $L = 1$ m; by increasing $\psi$ they become concave as it appears from Fig. 13 (M_uprights) and Fig. 14 (S_uprights), both related to the case $k = k_w = 1$ but are also adequately representative of all the considered cases.

## 7. Comparison between the design approaches

Only the direct comparison of the three approaches previously discussed in terms of the resistance domains allows to single out their differences: as examples, Figs. 15 and 16 present the non-dimensional domains associated with M_ and S_uprights, respectively, in case of $k = k_w = 1$ and $L = 3$ m. It is worth to mention that these figures are representative also for all the other cases, which have not been plotted, owing to the need of containing the length of the paper. It appears that the General Method defines the more favorable domain and the approach of EC3-1-3 is the more conservative, while the one associated with EN 15512 is always approximately in the middle. More comments are possible if a suitable parameter ($LCC^L$) is considered, which, with reference to the generic method (superscript $L$) can be defined (Fig. 17) as:

$$LCC^L = \sqrt{\left(n_{Rd}^L\right)^2 + \left(m_{Rd}^L\right)^2} \tag{15}$$

Table 3 is related to the approaches for cold-formed members and represents the $LCC^{15512}/LCC^{EC3\text{-}1\text{-}3}$ ratio for $k = k_w = 1$, excluding the limit cases ($e = 0$ and $e =$ ) because this ratio is equal to the unity, being both effective cross-section properties and relative slenderness independent from the design approach. It results that the rack procedure leads to a higher value of the load carrying capacity and maximum differences are approximately up to 18%, independently from the moment distribution, member slenderness and flexural–torsional restraints.

Attention has then been focused on the benefits associated with the use of the General Method and Tables 4 and 5 propose the $LCC^{G.M.}/LCC^{15512}$ and $LCC^{G.M.}/LCC^{EC3\text{-}1\text{-}3}$ ratios. Also in these cases data are related to $k = k_w = 1$ but these ratios are however suffi-ciently representative also for all the other values of $k$ and $k_w$. Fur-thermore, these data are plotted in Figs. 18–21 versus $\alpha_{ecc}$ that is the eccentricity angle ranging from 0 (only axial load, no bending moment) to $\pi/2$ (only bending moment, no axial load). Similarly, Figs. 22–25 refer to the relationship $LCC^{G.M.}/LCC^{EC3\text{-}1\text{-}3} - \alpha_{ecc}$. It should be noted that:

- a similar trend can be observed for all these data: each curve reaches a maximum value in the range 0–$\pi/8$, which corresponds to axial load eccentricities from 0 to 100 mm, typical values for uprights in semi-continuous sway frames;
- the greatest benefits can be observed in the load carrying capacity of the General Method with reference to the cases of non-uniform moments ($\psi = 0$ and $\psi = -1$);
- if reference is made to the comparison between the General Method and the EN 15512 approach (Table 4 and Figs. 18–21) load carrying capacity of the former is always greater than the latter: the ratio $LCC^{G.M.}/LCC^{15512}$ increases with the increasing of the member length being slightly dependent on the distribution of the applied moment. Maximum values of this ratio are in the range 1.20–1.25 except than for R_uprights, being the benefits associated with the use of the General Method slightly lower than 18%;
- as to the comparison between the General Method and the EC3-1-3 approach (Table 5 and Figs. 22–25), it can be noted that the maximum values of $LCC^{G.M.}/LCC^{EC3\text{-}1\text{-}3}$ ratio are up to 1.45, to confirm that the EC3-1-3 approach is the more conservative, despite overestimating the beam–column elastic buckling domain.

Furthermore, in order to have a general overview of these methods, the frequency and the cumulated relative frequency are plotted in Fig. 26 ($LCC^{15512}/LCC^{EC3\text{-}1\text{-}3}$), Fig. 27 ($LCC^{G.M.}/LCC^{15512}$) and Fig. 28 ($LCC^{G.M.}/LCC^{EC3\text{-}1\text{-}3}$), together with the associated 95% fractile value. With reference to $LCC^{15512}/LCC^{EC3\text{-}1\text{-}3}$ ratio, a non-negligible amount of values is greater than 1.10 (Fig. 26) confirming the non-equivalence between these two methods, as it appears also from the 95% fractile value approximately equal to 1.19. Furthermore, the benefits associated with the use of the General Method with respect to the EN 15512 approach are more limited than the ones obtained when the EC3-1-3 approach is

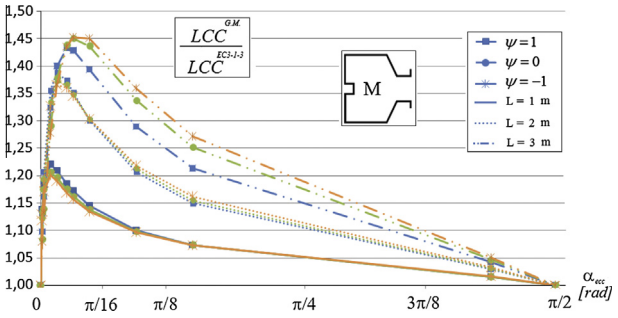


**Fig. 22.** $\frac{LCC^{G.M.}}{LCC^{EC3\text{-}1\text{-}3}} - \alpha_{ecc}$ relationships for the M_uprigths.

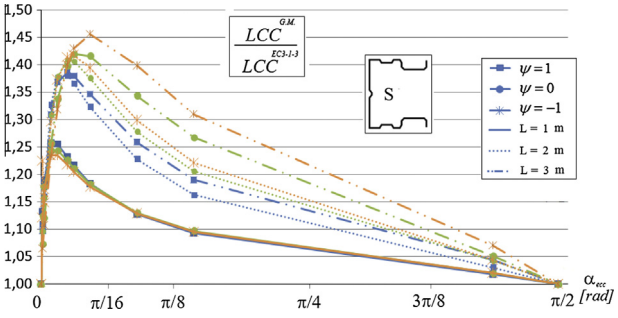


**Fig. 23.** $\frac{LCC^{G.M.}}{LCC^{EC3\text{-}1\text{-}3}} - \alpha_{ecc}$ relationships for the R_uprigths.

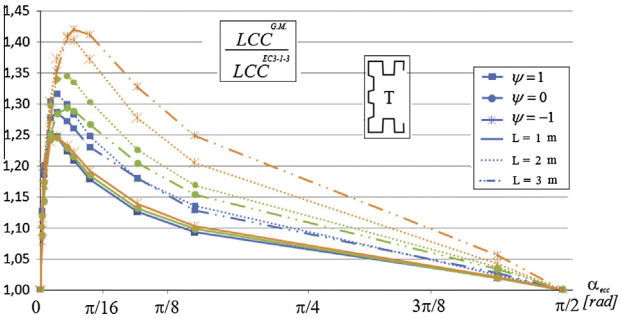


**Fig. 24.** $\frac{LCC^{G.M.}}{LCC^{EC3\text{-}1\text{-}3}} - \alpha_{ecc}$ relationships for the S_uprigths.

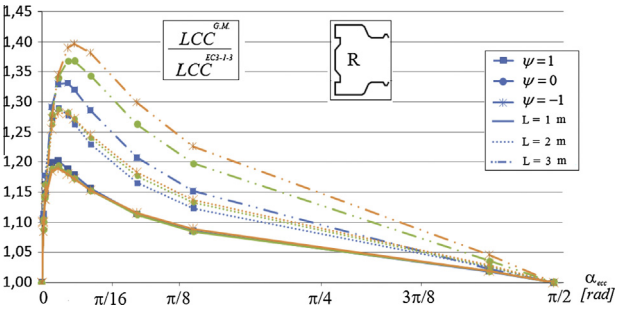


**Fig. 25.** $\frac{LCC^{G.M.}}{LCC^{EC3\text{-}1\text{-}3}} - \alpha_{ecc}$ relationships for the T_uprigths.

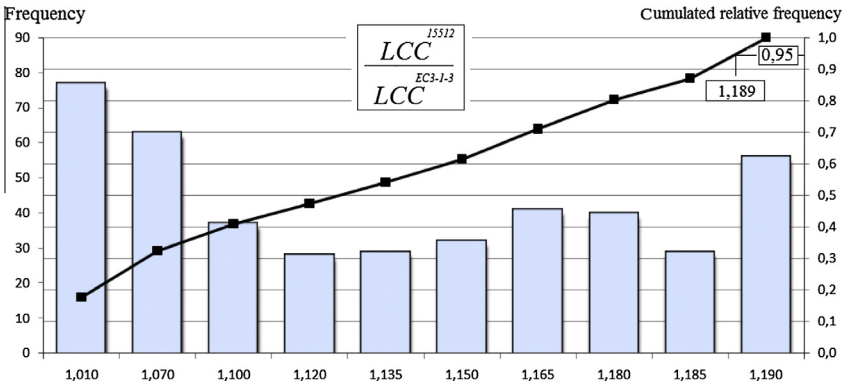


**Fig. 26.** Frequency and cumulated relative frequency distribution of $\frac{LCC^{15512}}{LCC^{EC3\text{-}1\text{-}3}}$ ratio for all the uprights with $k = k_w = 1$.

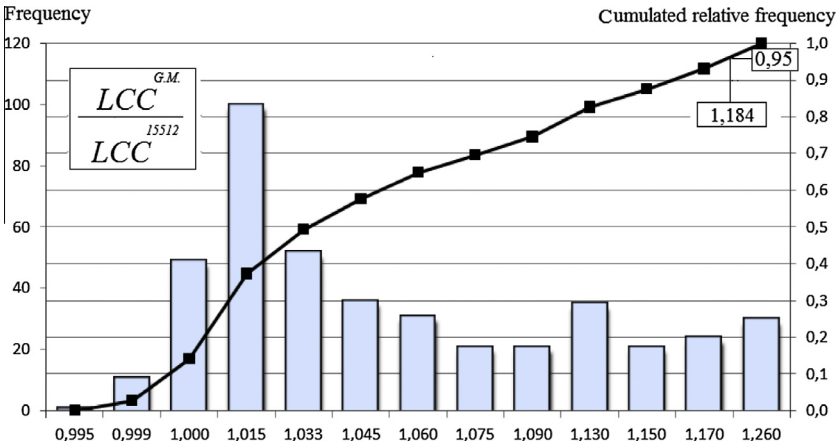


**Fig. 27.** Frequency and cumulated relative frequency distribution of $\frac{LCC^{G.M.}}{LCC^{15512}}$ ratio for all the uprights with $k = k_w = 1$.

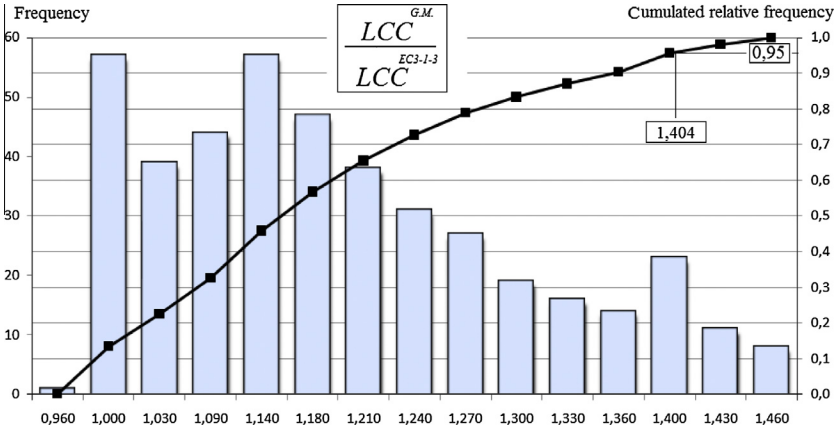


**Fig. 28.** Frequency and cumulated relative frequency distribution of $\frac{LCC^{G.M.}}{LCC^{EC3\text{-}1\text{-}3}}$ ratio for all the uprights with $k = k_w = 1$.

considered. In the first case, a great amount of data is in the range 1.00–1.08 and the 95% fractile value, equal to 1.18, is practically coincident with the one associated with the $LCC^{15512}/LCC^{EC3\text{-}1\text{-}3}$ ratio, despite the great differences in the data distribution. If load carrying capacity of the General Method is compared with the one of EC3-1-3, a non-negligible amount of data is located in a wider range, from unity to 1.30, approximately, and the 95% fractile value is significantly high (1.40, approximately).

## 8. Concluding remarks

Steel storage pallet rack uprights, which are thin-walled cold formed members, are usually subjected to axial load and gradient moment, being the loads sustained by the pallet beams, which transfer bending moment at their ends via semi-rigid connections. The upright design is quite fairly complex because of the interactions between the different forms of instability; their weight

directly reflects on the cost of the whole rack system and, as a consequence, on its competitiveness on the market. Three different design procedures have been discussed in the present paper, making reference to the European design rules considering the rack code [5], the part 1-3 of EC3 for cold-formed members [44] and the General Method described in part 1-1 of EC3 [45]. As discussed, a substantial difference is due to the way to take into account the buckling interaction between axial load and bending moments: only the latter (General Method) considers correctly the influence of the axial load on the buckling moment while the formers assume a non-conservative elastic buckling domain, as shown in Fig. 7.

Isolated members have been considered by selecting a wide range of design cases, differing for the cross-section geometry, member slenderness and load conditions. Class 3 uprights have been selected making reference to solid (no perforated) members. On the basis of a direct comparison of the load carrying capacity (LCC), it should be noted that the LCC values depend significantly on the adopted design method, with a non-negligible impact on the market. If reference is made to the codes properly recom-mended for cold formed rack members, the domains associated with the EN 15512 approach are more favorable than the one obtained via EC3 part 1-3 and differences are not negligible. Both these approaches need however urgent revision in order to take adequately into account the buckling interaction between axial load and bending moment occurring in beam–columns. This inter-action is however properly considered only in the General Method, which therefore leads to a remarkable increment of the member performances up to 23% and 45% if referred to the ones associated with the EN 15512 or with the EC3-1-3 approach, respectively. Fur-thermore, it is worth to mention that General Method appears also a very promising alternative design procedure if suitable software tools are available to evaluate the critical elastic buckling of uprights with regular systems of perforations, allowing hence avoiding the experimental phase necessary to evaluate the effec-tive cross-section properties.

Finally, it should be noted that the validity of the paper outcomes is related not only to all the storage systems employing uprights having cross-section similar to the ones in Fig. 2 but also for all structural systems made by mono-symmetric (solid) members. No attention has been paid to the design of perforated uprights, which has been investigated in a separate study [66].

## Appendix A. Prediction of the buckling of beam–column

The basic concepts of the theory of elastic stability of isolated members [11,30,39,45] are here shortly presented.

### A.1. Evaluation of the column buckling load

The elastic critical load for an isolated column ($N_{cr}$) is associated with the minimum value of the buckling load due the flexural ($N_{cr,y}$ and $N_{cr,z}$), torsional ($N_{cr,T}$), or flexural–torsional ($N_{cr,FT}$), buckling modes, which are defined as:

$$N_{cr,y/z} = \frac{\pi^2 E I_{y/z}}{\left(L_{y/z}\right)^2} \tag{A1}$$

$$N_{cr,T} = \frac{1}{i_0^2}\left[G \cdot I_t + \frac{\pi^2 E I_w}{L_T^2}\right] \quad with\ i_0^2 = \rho_y^2 + \rho_z^2 + y_0^2 \tag{A2}$$

$$N_{cr,FT(1,2)} = \frac{1}{2}\frac{N_{cr,y}}{1-\left(\frac{y_0}{i_0}\right)^2}\left[1+\frac{N_{cr,T}}{N_{cr,y}} \pm \sqrt{\left(1+\frac{N_{cr,T}}{N_{cr,y}}\right)^2 - 4\left(\frac{y_0}{i_0}\right)^2\frac{N_{cr,T}}{N_{cr,y}}}\right] \tag{A3}$$

where $E$ and $G$ are the elastic and shear moduli of the material, respectively, $L$ is the effective length for the pertinence buckling mode, $I_{y/z}$ are the second moments of area about the cross-section principal axes ($y$ or $z$), $I_t$ is the torsional coefficient, $I_w$ is the warping coefficient while $y_0$ expresses the distance between the shear center and the centroid along the $y$–$y$ axis, which (Fig. 4) is the symmetry axis of the cross-section.

In the expression (A3) the subscript notation (1, 2) indicates that flexural–torsional buckling load takes two different values, the lower of which has to be considered for the column buckling.

### A.2. Evaluation of the beam buckling moment [39,45]

The critical bending moment $M_{cr}^{B}$ of a mono-symmetric cross-section beam is given by:

$$M_{cr}^{B} = C_1\frac{\pi^2 E I_z}{(kL)^2}\left[\sqrt{\left(\frac{k}{k_w}\right)^2\frac{I_w}{I_z} + \frac{(kL)^2 G I_t}{\pi^2 E I_z} + \left(C_2 z_g - C_3 z_j\right)^2} - \left(C_2 z_g - C_3 z_j\right)\right] \tag{A4}$$

where terms $k_w$ and $k$ are suitably introduced to account for the restraints of the cross-section.

In particular, $k_w$ is an effective length factor accounting for warping end restraint, ranging from 0.5 (full fixity) to 1.0 (no fixity): $k_w = 0.7$ is recommended for one end fixed and the other end free; term $k$ is an effective length factor accounting for rotation: as for $k$ term, $k_w$ varies from 0.5 for full fixity to 1.0 for no fixity, with 0.7 for one end fixed and the other end free.

Term $z_g$ is the distance between the point of application of the load and the shear center and $z_j$ is a parameter defined as:

$$z_j = y_s - \frac{0.5}{I_y}\int_A (y^2 + z^2) z dA \tag{A5}$$

It can be noted that $z_j$ vanishes in case of double symmetric cross-section or when a critical moment acts about axis of symmetry: the Eq. (A4) can be re-written as:

$$M_{cr}^{B} = C_1\frac{\pi^2 E I_z}{(kL)^2}\left[\sqrt{\left(\frac{k}{k_w}\right)^2\frac{I_w}{I_z} + \frac{(kL)^2 G I_t}{\pi^2 E I_z}}\right] \tag{A6}$$

Coefficients $C_1$, $C_2$ and $C_3$ depend on the shape of the bending moment diagram (i.e. by the load conditions), and on the support conditions. Herein, attention is focused on members under gradient moment and hence only $C_1$ coefficients is of interest: its value is reported in Table A.1 for the considered design cases.

### A.3. Buckling of beam–columns

Reference has been in the following made to the cases of interest for routine rack design, i.e. Uprights under gradient moment (Fig. 6) about the symmetry axis (down-aisle direction of the rack).

The elastic critical moment of the beam ($M_{cr}^{B-C}$) can be obtained from the classical equation as:

$$M_{cr}^{B-C} = C_1\frac{\pi^2 E I_z}{(kL)^2}\left[\sqrt{\left[\left(\frac{k}{k_w}\right)^2\frac{I_w}{I_z} + \frac{(kL)^2 G I_t}{\pi^2 E I_z}\right]\cdot f(N) + \left(C_2 z_g - C_3 z_j\right)^2} - \left(C_2 z_g - C_3 z_j\right)\right] \tag{A7a}$$

**Table A.1**
Values of $C_1$ proposed by Ref. [36].

| Bending moment gradient ($\psi$) | Restrain condition ($k$) | | |
|---|---|---|---|
| | 1.0 | 0.7 | 0.5 |
| *C1 coefficient* | | | |
| $\psi = 1$ | 1.000 | 1.000 | 1.000 |
| $\psi = 0$ | 1.879 | 2.092 | 2.150 |
| $\psi = -1$ | 2.752 | 3.063 | 3.149 |

where all the terms are already discussed with exception of function $f(N)$, depending on the level of the acting axial load, that is defined as:

$$f(N) = \left(1 - \frac{N}{N_{cr,y}}\right)\left(1 - \frac{N}{N_{cr,FT(1)}}\right)\left(1 - \frac{N}{N_{cr,FT(2)}}\right) \tag{A7b}$$

For the considered cases the Eq. (A7a) becomes:

$$M_{cr}^{B-C} = C_1 \frac{\pi^2 EI_z}{(kL)^2}\left[\sqrt{\left[\left(\frac{k}{k_w}\right)^2 \frac{I_w}{I_z} + \frac{(kL)^2 GI_t}{\pi^2 EI_z}\right] \cdot f(N)}\right] = M_{cr}^{B-C} = M_{cr}^{B} \cdot \sqrt{f(N)} \tag{A8}$$

## Appendix B. List of symbols

Latin lower case letters

$d$ = distance between the centroid and the web.
$f$ = generic function, yielding stress.
$e$ = eccentricity.
$k$ = restraint condition.
$m$ = non-dimensional bending moment.
$n$ = non-dimensional axial load.
$u$ = displacement along $x$ axis.
$v$ = displacement along $y$ axis.
$w$ = displacement along $z$ axis.
$x$ = longitudinal axis of the beam.
$y$ = symmetry axis of the cross-section.
$z$ = non symmetry axis of the cross-section.

Latin upper case letters

$B$ = bi-moment.
$C$ = coefficient.
DOF = degrees of freedom.
$E$ = Young's modulus.
$F$ = shear force.
FE = finite element.
$G$ = shear modulus.
$I$ = second moment of area.
$L$ = length.
LCC = load carrying capacity.
$M$ = moment.
$N$ = axial force.
$W$ = section modulus.

Greek lower case letters

$\alpha$ = load multiplier, angle.
$\beta$ = equivalent uniform moment factor.
$\gamma$ = safety factor.
$\chi$ = reduction factor.
$\varphi$ = rotation.
$\lambda$ = slenderless.
$\theta$ = warping function.
$\rho$ = radius gyrator of inertia.
$\omega$ = sectorial area.
$\psi$ = gradient moment.

Subscripts

*b* = beam.
*cr* = critical.
*ecc* = eccentricity.
*Ed* = design value.
*eff* = effective.
*FT* = flexural–torsional buckling.
*inf* = low value of section modulus.
*j* = end node of the beam element, joint.
*i* = end node of the beam element.
*LT* = lateral torsional buckling.
*M* = material.
max = maximum.
min = minimum.
*o* = position of the centroid.
*op* = optimal.
*Rd* = resistance value.
*Rk* = characteristic resistance.
*s* = position of the shear center.
*sup* = upper value of section modulus.
*t* = Saint Venant's torsion.
*ult* = ultimate.
*w* = warping.
*x* = longitudinal axis of beam element.
*y* = symmetry axis of the cross-section, yielding of the material.
*z* = non symmetry axis of the cross-section.
$\omega$ = sectorial area.

Superscripts

15512 = term related to the application of the EN 15512.
*B* = beam.
*B–C* = beam column.
EC3-1-3 = term related to the application of the EC3-1-3.
*G.M.* = term related to the application of the EC3-1-1.
*L* = suitable term.
*LTBeam* = term related to application of LTBeam FE software.
*Siva* = term related to application of Śiva FE software.
*th* = term related to application of theory's procedure.

## References


[1] Shafer BW. Cold-formed steel structures around the world – a review of recent advances in applications, analysis and design. Steel Constr 2011;4:141–9.
[2] Godley MHR. In: Rhodes, editor. Design of cold formed steel members. Elsevier Applied Science; 1991. p. 361–99.
[3] Takeuchi T, Suzuki K. Performance-based design for truss-frame structures using energy dissipation devices. In: Mazzolani FM, editor. Proceedings, STESSA 2003. p. 55–61.
[4] ECCS – European Convention for Structural Steelworks. Analysis and design of steel frames with semi-rigid joints, Publication No. 67; 1992.
[5] CEN, EN 15512. Steel static storage systems – adjustable pallet racking systems – principles for structural design. CEN European Committee for Standardization; 2009. p. 137.
[6] RMI, MH 161. Specification for the design, testing and utilization of industrial steel storage racks. RMI – Rack Manufacturers Institute; 2008. p. 59.
[7] Australian Standards, AS 4084 – steel storage racking. AS Standards, Australia; 2012.
[8] FEM 10.2.08. Recommendations for the design of static steel storage pallet racks in seismic conditions. Federation Européenne de Manutention, version 1.00; 2010.
[9] FEMA 460. Seismic considerations for steel storage racks located in areas accessible to the public. Prepared by the Building Seismic Safety Council for the Federal Emergency Management Agency; 2005.
[10] CEN, prEN 16681. Steel static systems – adjustable pallet racking systems – principles for seismic design. CEN European Committee for Standardization; 2013.
[11] Chen WF, Atsuta T. Theory of beam–columns: space behaviour and design, vol. 2. McGraw Hill; 1977.
[12] Conci A, Gattass M. Natural approach for geometric non-linear analysis of thin-walled frames. Int J Numer Methods Eng 1990;30:207–31.
[13] Hsiao KM, Lin WY. A co-rotational formulation for thin-walled beams with monosymmetric open section. Comput Methods Appl Mech Eng 2000;190:1163–85.
[14] Teh LH. Cubic beam elements in practical analysis and design of steel frames. Eng Struct 2001;23:1243–55.

[15] Battini JM, Pacoste C. Co-rotational beam elements with warping effects in instability problems. Comput Methods Appl Mech Eng 2002;191:1755–89.
[16] Turkalj G, Brnic J, Prpic-Orsic J. Large rotation analysis of elastic thin-walled beam-type structures using ESA approach. Comput Struct 2003;81:1851–64.
[17] Chen HH, Lin WY, Hsiao KM. Co-rotational finite element formulation for thin-walled beams with generic open section. Comput Methods Appl Mech Eng 2006;195:2334–70.
[18] El Fatmi R. Non-uniform warping including the effects of torsion and shear forces. Part I: A general beam theory. Int J Solids Struct 2007;44:5912–29.
[19] Saritas A. Modeling of inelastic behavior of curved members with a mixed formulation beam element. Finite Elem Anal Des 2009;45:357–68.
[20] Nascimbene R. An arbitrary cross section, locking free shear-flexible curved beam finite element. Int J Comput Methods Eng Sci Mech 2013;14:90–103.
[21] Attard MM. Lateral buckling analysis of beams by the FEM. Comput Struct 1986;23(2):217–31.
[22] Mohri F, Damil N, Potier-Ferry M. Large torsion finite element model for thin-walled beams. Comput Struct 2008;86:671–83.
[23] Erkmen RE, Mohareb M. Buckling analysis of thin-walled open members – a finite element formulation. Thin Walled Struct. 2008;46:618–36.
[24] Dourakopoulos JA, Sapountzakis EJ. Postbuckling analysis of beams of arbitrary cross-section using BEM. Eng Struct 2010;32:3713–24.
[25] Bathe K, Wilson EL. Numerical methods in finite element analysis. Prentice-Hall; 1976.
[26] Werkle H. Finite element in der Baustatik. Vieweg; 2008.
[27] Zienkiewicz OC, Taylor RL. The finite element method. Butterworth Heinemann; 2000.
[28] ConSteel 7.0. Finite-element-program. Consteel Solutions Ltd. <http://www.consteel.hu>.
[29] ABAQUS/STANDARD user's manual version 6.8. Hibbit, Karlsson and Sorensen, USA; 2006.
[30] LS-DYNA. <http://www.ls-dyna.com/1_pages/1lsdyna.htm>.
[31] The SOFiSTiK FEM packages. <http://www.sofistik.com/en/>.
[32] ANSYS. <http://www.Ansys.com>.
[33] Teh LH, Hancock GJ, Clarke MJ. Analysis and design of double sided high-rise steel pallet rack frames. J Struct Eng 2004;130:1011–21.
[34] Gilbert BP, Rasmussen KJR. Drive-in steel storage racks I: stiffness test and 3D load transfer mechanisms. ASCE J Struct Eng 2012;138(2):135–47.
[35] Bernuzzi C, Pieri A, Squadrito V. Warping influence on the monotonic design of unbraced steel storage pallet racks. Thin Walled Struct 2014;79:71–82.
[36] Bernuzzi C, Gobetti A, Gabbianelli G, Simoncelli M. Warping influence on the resistance of uprights in steel storage pallet racks. J Constr Steel Res 2014;101:224–41.
[37] Bernuzzi C, Gobetti A, Gabbianelli G, Simoncelli M. Unbraced pallet rack design in accordance with European practice. Part 2: Essential verification checks. Thin Walled Struct 2015;86:208–29.
[38] Trahair NS. Flexural–torsional buckling of structures. London E & F Spon; 1993.
[39] Teh LH. Beam element verification for 3D elastic steel frame analysis. Comput Struct 2004;82:1167–79.
[40] Bathe KJ, Wilson EL, Iding RH. NONSAP-finite element calculation for nonlinear static and dynamic analysis of complex structures. Berkeley, California, USA: Structural Engineering Laboratory, University of California; 1978.
[41] Bernuzzi C, Gobetti A. A curved beam finite element for the structural analysis of skeleton frames with non-symmetric members. Part 1: the linear formulation. Costruzioni Metalliche [submitted for publication].
[42] Bernuzzi C, Gobetti A, Gabbianelli G, Simoncelli M. Śiva-system of incremental and vibration analysis: software for a finite element analysis for beam with warping influence [in preparation].
[43] Mohri F, Brouki A, Roth JC. Theoretical and numerical stability analyses of unrestrained, mono-symmetric thin-walled beams. J Constr Steel Res 2003;59:63–90.
[44] European Committee for Standardization. CEN, Eurocode 3 – design of steel structures – Part 1-3: Design of cold formed members, CEN, Brussels; May 2005.
[45] CEN. Eurocode 3 – design of steel structures – Part 1-1: General rules and rules for buildings. CEN European Committee for Standardization; 2005.
[46] Timoshenko SP, Gere JM. Theory of elastic stability. 2nd ed. New York: McGraw Hill; 1961.
[47] Vlasov VZ. Thin walled elastic beams. 2nd ed. Jerusalem: Israel Program for Scientific Transactions; 1961.
[48] Serna MA, Lopes A, Puente I, Yong DJ. Equivalent uniform moment factors for lateral torsional buckling of steel members. J Constr Steel Res 2006;62(6):566–80.
[49] Mohri F, Damil N, Potier-Ferry M. Buckling and lateral buckling interaction in thin-walled beam–column elements with mono-symmetric cross sections. Appl Math Model 2013;37:3526–40.
[50] Kekova Y, Balaz B. In: Ivany M, editor. Critical moments, stability and ductility of steel structures. Academiai Kiado, Budapest; 2002.
[51] CEN, ENV 1993-1-1. Eurocode 3 – design of steel structures, Part 1-1: General rules and rules for building. CEN European Committee for Standardization; 1992.
[52] Trahair NS, Woolcock ST. Effect of major axis curvature on I-beam stability. J Eng Mech Div ASCE 1973;99(1):85–98.
[53] Machado SP. Interaction of combined loads on the lateral stability of thin-walled composite beams. Eng Struct 2010;32:3516–27.
[54] Mohri F, Bouzerira C, Potier-Ferry M. Lateral buckling of thin-walled beam–column elements under combined axial and bending loads. Thin-Walled Struct 2008;46:290–302.
[55] Sangle KK, Bajoria KM, Talicotti RS. Elastic stability analysis of cold-formed pallet rack structures with semi-rigid connections. J Constr Steel Res 2012;71:245–62.
[56] Bajoria KM, Sangle KK, Talicotti RS. Modal analysis of cold-formed pallet rack structures with semi-rigid connections. J Constr Steel Res 2010;66(3): 428–41.
[57] LTBEAM. <https://www.cticm.com/content/ltbeam-version-1011>.
[58] Hughes A. Getting the best out of LTBeam. <http://www.steelconstruction.org/index.php?option=com_documents&task=downloadDocument&doc=49295&file=53935>.
[59] Boissonnade N, Greiner R, Jaspart JP, Lindner J. Rules for member stability in EN 1993-1-1 background documentation and design guidelines. ECCS – European Convention for Structural Steelworks, Publication No. 119; 2006.
[60] Bernuzzi C, Rugarli P. A unified approach for the design of columns and beam–columns cold-formed members. Part 1: The approach. COSTRUZIONI METALLICHE No. 5; 2009 [in English].
[61] Bernuzzi C, Rugarli P. A unified approach for the design of columns and beam–columns cold-formed members. Part 2: Validation of the approach. COSTRUZIONI METALLICHE No. 6; 2009 [in English].
[62] Bijlard F, Feldmann M, Naumes J, Sedlacek G. The "General Method" for assessing the out-of-plane stability of structural members and frames in comparison with alternative rule in En 1993 – Eurocode 3 – Part 1-1. Steel construction, vol. 3, No. 1. Ernst & Sohn ed.; 2010.
[63] Szalai J. The "General Method" of EN 1993-1-1. NSC April 11. p. 30–1.
[64] Papp F. Global stability analysis using "General Method". <www.consteelsoftware.com/files/sharedUploads/Pdf/General_stability_analysis.pdf>.
[65] Castiglioni CA, Kanyilmaz A, Angeretti M, Brambilla G, Chiarelli GP, Bernuzzi C. Experimental results of full scale push over tests of project SEISRACK2 (seismic behaviour of steel storage pallet racking systems). In: 2nd European conference on earthquake engineering, Istanbul, August 25–29, 2014.
[66] Bernuzzi C, Maxenti F. European alternatives to design perforated thin-walled cold-formed beam–columns for steel storage rack systems. J Constr Steel Res [submitted for publication].